

Green hydrogen techno-economic assessments from simulated and measured solar photovoltaic power profiles

Nicolas Campion ^{a,*¹}, Giulia Montanari ^{b,1}, Alessandro Guzzini ^c, Lennard Visser ^d, Alfredo Alcayde ^e

^a Department of Management, Technical University of Denmark, Produktionstorvet, 424, 008, 2800, Kgs. Lyngby, Denmark

^b Department of Energy, Politecnico di Torino, Corso Duca degli Abruzzi 24, 10129, Torino, Italy

^c Department of Industrial Engineering, University of Bologna, viale del Risorgimento 2, 40136, Bologna, Italy

^d Copernicus Institute of Sustainable Development, Utrecht University, Princetonlaan 8a, 3584 CB, Utrecht, the Netherlands

^e Department of Engineering, Universidad de Almería, Crtra. Sacramento s/n., 04120, Almería, Spain



ARTICLE INFO

Dataset link: [OptiPlant \(Original data\)](#), [Measured-vs-simulated-PV \(Original data\)](#)

Keywords:
Green hydrogen
Solar PV
e-fuels
Reanalysis
Simulation
Power measurements
Techno-economic

ABSTRACT

Studies estimating the production cost of hydrogen-based fuels, known as e-fuels, often use renewable power profile time series obtained from open-source simulation tools that rely on meteorological reanalysis and satellite data, such as Renewables.ninja or PVGIS. These simulated time series contain errors compared to real on-site measured data, which are reflected in e-fuels cost estimates, plant design, and operational performance, increasing the risk of inaccurate plant design and business models. Focusing on solar-powered e-fuels, this study aims to quantify these errors using high-quality on-site power production data. A state-of-the-art optimization techno-economic model was used to estimate e-fuel production costs by utilizing either simulated or high-quality measured PV power profiles across four sites with different climates. The results indicate that, in cloudy climates, relying on simulated data instead of measured data can lead to an underestimation of the fuel production costs by 36 % for a hydrogen user requiring a constant supply, considering an original error of 1.2 % in the annual average capacity factor. The cost underestimation can reach 25 % for a hydrogen user operating between 40 % and 100 % load and 17.5 % for a fully flexible user. For comparison, cost differences around 20 % could also result from increasing the electrolyser or PV plant costs by around 55 %, which highlights the importance of using high-quality renewable power profiles. To support this, an open-source collaborative repository was developed to facilitate the sharing of measured renewable power profiles and provide tools for both time series analysis and green hydrogen techno-economic assessments.

1. Introduction

As concerns about climate change and security of energy supply are increasing, more and more attention is geared toward hydrogen based fuels produced from renewable electricity. Indeed, these fuels, also referred as “e-fuels” seem to have the potential to reduce the greenhouse gas emissions of various sectors that are difficult to electrify such as aviation, shipping or hard to abate industry [1]. In the past years, a large number of studies were conducted to propose optimized process design for e-fuel production and cost estimations [2–6], and how to integrate e-fuel into future energy systems [7–12]. Due to their low cost, technology readiness level, and widespread resources, most studies have

been focusing on techno-economic assessments of e-fuels produced via solar and wind energy [6,13–18]. In these studies, wind and solar power time series are commonly obtained with tools using satellite or reanalysis data, like the open-source tool Renewables.ninja [19] as shown in Table 1.

Although site level inaccuracies of these tools compared to ground measured data is already well discussed and understood in the field of reanalysis and renewable time series generation [39–43], studies focusing on power-to-X techno-economic assessment usually not address this issue. In general, the quality of the solar data used is not extensively discussed, the influence of using other weather datasets or PV power calculation methods is not tested, and the sensitivity analyses are usually conducted for other uncertain parameters. Some studies [22,30] did

* Corresponding author.

E-mail address: njbc@dtu.dk (N. Campion).

¹ Contributed equally to the work of this study.

| Nomenclature | | |
|----------------------|---|--|
| Abbreviations | | |
| AC | Alternating current | CF_i^{sim} Simulated capacitor factor per period i |
| c-Si | Crystalline silicon | CF_i^{meas} Measured capacity factor at the experimental plant per period i |
| CdTe | Cadmium telluride | CF^{diff} Annual average capacity factor difference |
| CIS | Copper indium gallium selenide solar cel | Cons_u Consumption (when negative) or the production (when positive) of electricity or hydrogen of a unit u |
| CorRES | Correlations in Renewable Energy Sources | D_u Yearly fuel production target |
| DC | Direct current | F_u Fixed O&M costs |
| ECMWF | European center for medium-range weather forecasts | I_u Investment expenditure of unit u |
| ERA | European Centre for Medium-Range Weather Forecasts Reanalysis | In_j Subset of units used to charge a tank |
| LCOA | Levelized Cost of Ammonia | L_u^{min} Minimum load |
| LCOF | Levelized Cost of Fuel | MAE Mean Absolute Error |
| MERRA | Modern-Era Retrospective analysis for Research and Applications | Min Minimum |
| NSRDB | National Solar Radiation Database | MinD Subset of units required to produce the end-fuel |
| PV | Photovoltaic | n Number of hours simulated and measured per year |
| PVGIS | Photovoltaic Geographical Information System | Out _i Subset of units used to discharge a tank |
| SARAH | The Surface Solar Radiation Data Set - Heliosat | P_i Subset of units synthesizing a product using a reactant |
| SSE | Surface meteorology and Solar Energy | $P_{u,t}$ Hourly price of the output from unit u at time t |
| STC | Standard test conditions | PP _{u,t} Normalized power profile of the unit u at time t |
| WACC | Weighed average cost of capital | RMSE Root Mean Square Error |
| Symbols | | T _i Subsets of units behaving like a tank |
| A _u | Annuity factor | V _u Variable O&M costs |
| c _u | Installed capacity of unit u | x _{u,t} Output flow of mass or energy from unit u at time t |
| | | ρ_{in} Charging efficiency of unit u |
| | | ρ_{out} Discharging efficiency of unit u |
| | | Ψ Subset of intermittent power units |

investigate the influence of choosing different weather years and showed that it has a significant effect on costs and system design for islanded systems, while being less significant for systems that are also grid connected since in the latter electricity price uncertainties play a larger role. This result highlights the importance of further investigating the methods and data used to generate the renewable power time series and the corresponding impact on the techno-economic assessment results, especially for islanded production systems.

Kies et al. [44] studied how using different meteorological datasets to derive renewable generation profiles influences the optimal design of the European power system. It was found that the selection of a dataset highly influences the system design and the electricity cost estimates

with differences around 10 %. Mathews et al. [45] analysed the bias in reanalysis derived solar profiles using the Supervisory Control And Data Acquisition (SCADA) data obtained from electricity market operators. They studied the error propagation occurring in energy system modeling studies where long duration energy storage is considered (for example hydrogen storage). It was found that MERRA-2 dataset tends to globally overestimate solar PV power output while ERA-5 showed better performances. In addition, it has been demonstrated that, particularly in cloudy climates, the error propagation caused by biases in the solar PV power profile is significant in energy systems that include long-duration hydrogen storage. While the few existing studies on this topic provide valuable contributions, none of them use high-resolution,

Table 1

Literature review of selected e-fuels techno-economic assessment studies and method used for PV power profile simulation.

| Ref. | E-fuel analysed | Tool used to calculate solar power profile | Weather dataset | Type of dataset | Sensitivity analysis on PV power time series |
|--------------------------|-----------------|--|---|--|---|
| [5,6,17, 20] [15] | Ammonia | Renewables.ninja | MERRA2 | Reanalysis | No |
| [22] | Ammonia | PVLib | ERA-5 | Reanalysis | Different weather years tested (2017–2019) |
| [23] [25] | Ammonia | No tool specified Used a simple formula | Meteonorm [24] ^a “Radiación solar” [26] | Satellite, ground station Satellite, ground station | No No |
| [27,28] [2] | Methanol | Renewables.ninja Own calculation method | MERRA2 NSRDB [29] | Reanalysis Satellite, reanalysis, ground station | No Solar PV orientation |
| [30] | Hydrogen | PVLib/PVGIS | Meteostat PVGIS [31] | Ground station, satellite | Different weather years tested (2007–2016) |
| [32] - [13] - [14] | Hydrogen | Own calculation method -Simple formula -TRNSYS software ^a | PVGIS Meteonorm ^a | Satellite, reanalysis Satellite, ground station | No No |
| [33–36] [37] | Hydrogen | Renewables.ninja ([33] added correction factors) Renewables.ninja, NASA [38], PVGIS and own calculation method (including correction factors) | MERRA2 MERRA2 | Reanalysis Reanalysis | No Different years considered (data from 1981 to 2021) |

^a Not open source.

ground-measured PV power data to calculate error propagation in the techno-economic assessment of power-to-X plants. This lack of validation in literature can partially be explained by the limited availability of high-resolution ground measured power data, which are either non-existent, not publicly accessible, or difficult to access. However, the use of high resolution PV measured data allows to identify error factors that are probably not detectable with a weather station or reanalysis data like for example dust, pollution, or the state of the solar panels (surface temperature, cleanliness). In addition, no study provides an open-source and accessible framework for both PV power time series analysis and power-to-X plant techno-economic assessment. Therefore, the aim of this work is to provide such an open-source framework to identify and quantify the impact of inaccuracies in power time series on the techno-economic assessments of hydrogen-based fuel. To do so, this research uses a state-of-the-art techno-economic model for hydrogen production fed with high-quality ground measured data or simulated solar PV power data and compare the results obtained in these two cases for four different sites/case studies. As a result, we give an order of magnitude of the error propagation that can be expected from the renewable time series imprecisions and compare it with typical other sources of error like electrolyser efficiency, financial assumptions or power-to-X plant component costs. The techno-economic assessment method adopted in this study uses an open-source state-of-the-art power-to-X plant investment and operation optimization model (Opti-plant) presented in Ref. [6]. The high-quality ground-measured PV power data used in this study are collected at four sites (Forlì and Turin in Italy, Utrecht in the Netherlands and Almería in Spain) with different weather variety and climates to give preliminary insights for result generalization. The framework developed for the techno-economic assessment, the power time series analysis and the input data are also made open-access to leave the possibility to replicate the study in other sites with high-quality measurements and complement the results obtained in this work [46,47].

The paper is structured as follows. In Section 2, the methods are explained, including site selection, on-site PV plants' power measurement and simulation, the assumptions on end-users' hydrogen profile, and techno-economic parameters implemented in the e-fuel plant's design optimization model. In Section 3, the results on the influence of weather and PV power quality data on e-fuels plants' design optimization are shown and discussed. Finally, conclusions and recommendations are provided in Section 4.

2. Method

The method section comprises a detailed description of the PV plant experimental set-up in the different measurement's sites (Forlì, Turin, Utrecht and Almería), a section describing how the different simulated PV power profile have been generated for the different sites, and finally a description of the optimization techno-economic assessment model used in this study.

2.1. Overview

As presented in Fig. 1, one aspect of the methodology involves comparing the characteristics of simulated time series with those measured on-site at the PV plant. Various tools and databases are employed to generate the simulated power profile time series to understand the power output differences related to reanalysis databases or PV power calculation methods. The second phase of the analysis involves utilizing these different time series in an e-fuel plant techno-economic optimization model. This aims to assess how errors in the original time series propagate into the evaluation of e-fuel costs and system sizing.

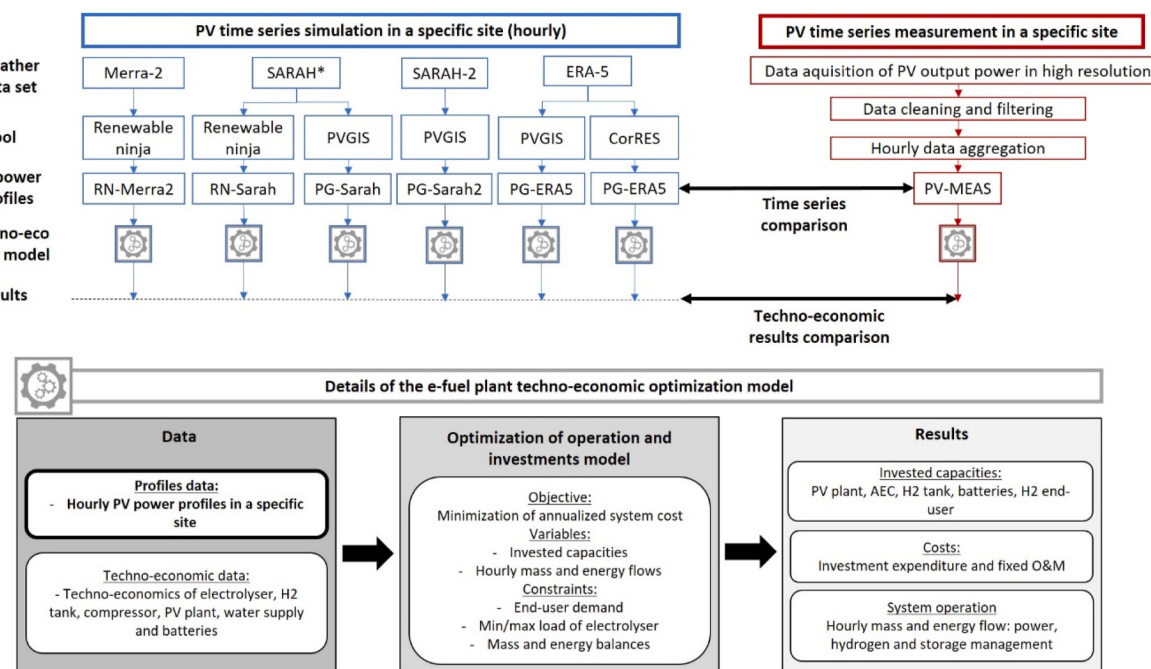


Fig. 1. Paper methodology.

2.2. Sites selection and description

As shown in Fig. 2, four different sites with a PV-plant and measurement system are selected for this study: Almería (Spain), Forlì, Turin (Italy), and Utrecht (the Netherlands). Each site presents different weather and climates conditions giving the possibility to partially generalize the results to other locations with similar features.

The first site is the applied research center on renewable energy called “HEnergia” (HE) in Forlì (Italy, 44°13'21" N- 12°02'27" E), where the measurements were made by the Department of Industrial Engineering of the University of Bologna in collaboration with the local multi-utility HERA S.p.a. The second site is the rooftop of the university Politecnico di Torino in Italy (Italy, 45°3'54" N- 7°39'32" E). Following the Köppen-Geiger climate classification [49], the climate in both Turin and Forlì can be described as humid subtropical climate (Cfa) characterized by hot and humid summers, and cool and damp winters. Locations with the same climates classification can be observed for example in the Australian East-coast (Queensland), American gulf and lower East-coast states in the US, or in Southern Brazil, north Argentina and Uruguay [50].

The third site is a mounted rooftop residential PV system in the region of Utrecht in the Netherlands taken from the open-source PV measurement database presented in Visser et al. [51]. The data base contains measurements from 175 different PV sites, based on the system orientation and data availability, System ID002 (approximately located at 51°9'01" N-5°32'17" E) was selected for the main analysis. The climate in the Netherlands can be characterized as temperate oceanic climate (Cfb) featured by warm summer and cool winters. This type of climate is typically characterized by frequent cloudy conditions and rain precipitations. Locations with the same climate classification are for example Western Europe, Southern Chile, or New Zealand.

The last site is a new solar power plant that was commissioned in February 2023 in Almería (Spain, 36° 55' 51" N - 2° 28' 18" W), with an installed capacity of 3.8 MW, directly connected to the grid. The climate classification of Almería is between a hot semi-arid and a hot desert climate (BSh/BWh) and is known to be one of the driest cities in Europe. The PV plant itself is located in a climate area qualified as hot desert (BWh). Hot desert climate can be found, among other places, in the deserts of Northern and Southern Africa (i.e. Sahara and Kalahari Desert), West-Asia (i.e. Arabian Desert), South Asia (in Iran, Pakistan and north India), Australia, or the coast of Chile and Peru. This type of climate usually presents clear sky and very high potential for solar power production [48].

The open-source collaborative repository [46] developed as part of this study can be used to share high-quality solar PV measurement data from other sites and climates.



Fig. 2. Sites selected for the study and specific photovoltaic power output [48].

2.3. On site PV-plant power measurement

This section presents the PV plant and experimental set-up for power output measurements at the selected locations.

2.3.1. PV plant set-up and measurements in Forlì, Italy (Cfa)

The on-site experimental PV plant consists in 8 different PV plants installed in 2013 that were experimentally assessed in Ref. [52]. This study focuses on the polycrystalline (poli c-Si) technology which is today the “default” technology usually applied in energy system models. The solar panels are installed with a fixed support on a roof with an inclination angle (tilt) of 30° and an azimuth of 180° (South-exposed). A string feeds energy via standard inverter into the grid and it is monitored and logged on the direct current (DC) and alternating current (AC) side of the inverter. The solar PV plant is connected to the grid through a Power One inverter, model Aurora 3.0. The poli c-Si PV panels have a module efficiency of 14.7 % at standard test conditions (STC) and occupy an area of 14.73 m². The total installed power is 2.16 kW at STC. Due to the small plant scale, the measured output power does not account for losses that would be greater in large-scale PV plants, such as shading, soiling, wiring, temperature losses, or lower inverter efficiencies. For consistency, these losses will not be counted either when simulating the PV power profiles in Forlì. The inverter losses in the experimental plant are measured around 95 %. The monitoring activities are done in accordance with the international standard IEC 61724. For every string, current and voltage (DC Wattmeter Electrex Femto) are monitored on the DC side. The power on the AC side of the inverter (AC Wattmeter Electrex Femto) is also measured. Moreover, each PV plant is equipped with a PT100 temperature sensor (Omega SA1-RTD-4W-120), installed on the rear of one of the plant modules. Furthermore, environmental conditions such as solar global radiation (Kipp & Zonen pyranometer CMP11), ambient temperature and humidity (LSI Lastem thermohygrometric sensor DMA675), wind speed and direction (LSI Lastem wind speed and direction sensor DNA721) are measured through a local meteorological station, installed on the roof. Each sensor produces signals in 4–20 mA. Signals coming from the PV plants are sent to the datalogger, while signals coming from the local meteorological station are sent to a dedicated datalogger. Data are acquired and stored every 4–5 s in a PC from the dataloggers via LAN network. Data are managed through MySQL Workbench on a PC that can be remotely accessed via internet. The data processed in this analysis have been recorded between the October 3, 2014 and the September 24, 2015. The architecture of the data acquisition system is shown with more details in Ref. [52]. The acquired data contains erroneous values that are due to temporary sensor, system defaults, or at some point plant electrical blackouts that deactivated the acquisition system. Erroneous data points contain missing data or unexpected null values. Identifying missing data is also straightforward as the measurement date is missing when the data acquisition system is off. The identification of null values is done by comparing the PV plant power output with the data from the meteorological station also present on-site or another PV plant on the experimental site. If the direct normal irradiance measured on the meteorological station is positive or the other PV plants are producing while the selected PV plant power production is null, the data point is replaced by a “missing” value. The value of the AC power output is measured at every data point and hourly aggregated calculating the average power produced every hour. If less than 60 data points are recorded in an hour (less than one point per minute), the hour is counted as “missing” when doing the hourly time aggregation. When running the techno-economic model, the missing values are replaced with values from a simulated time series (Renewables.ninja MERRA2) to avoid the use of zero values. This data substitution for some of the missing values will lead to an underestimation of the absolute error. In the measured time series, 12 % of the data are missing, mostly during spring and summer as it can be seen in Fig. 3.

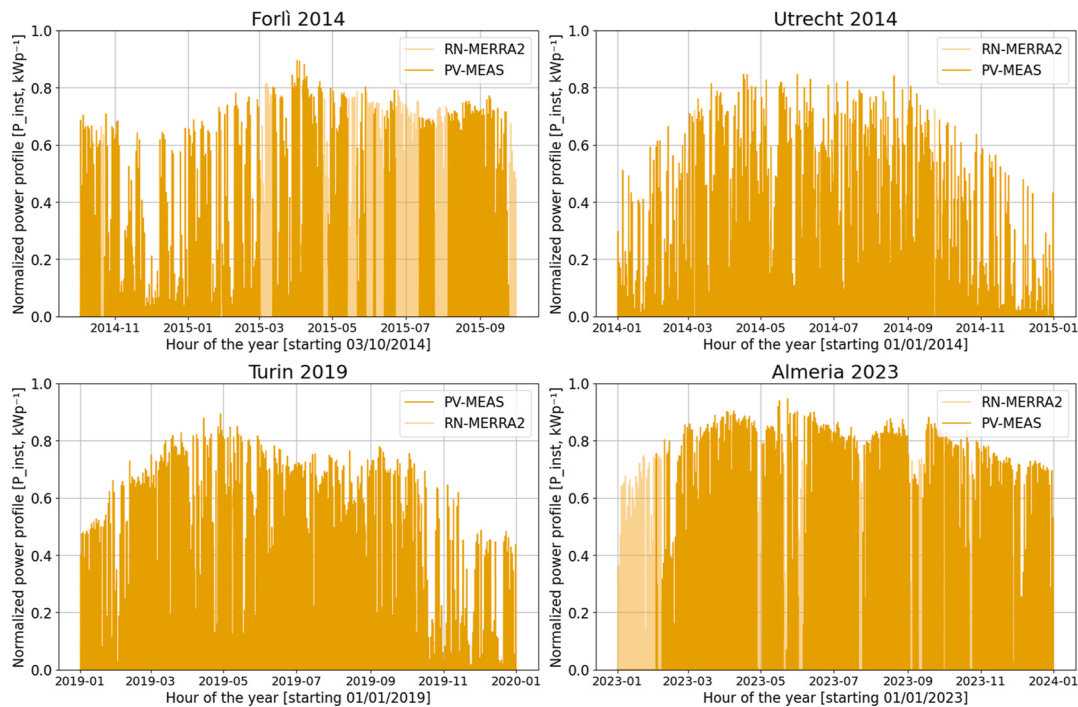


Fig. 3. Measured PV solar power time series in the four different sites and missing data.

2.3.3. PV plant set-up and measurements in Turin, Italy (Cfa)

The experimental PV plant consists in photovoltaic panels installed with a fixed support that is coplanar with a rooftop of the university Politecnico di Torino in Turin, Italy. The plant has been installed in 2018, while the period considered by the study is between January 1, 2019 and December 31, 2020. The period was chosen to compare the measured data with dataset like SARAH2 and ERA5. The plant has an inclination angle (tilt) of 26° as the rooftop and an azimuth of 206° (South-West exposed). The solar panels installed are Monocrystalline Benq (SunForte PM096B00) with an efficiency of 20.1 % at STC. There are 27 inverters Sunny Tripower between 20 and 25 kW (20000 TL/25000 TL) with an efficiency of 98 %. The power of each module is 327 W, the overall installed power is 604 kW, with a net occupy area of 3000 m². The data analysed consists of energy produced by the photovoltaic panels and recorded on the AC side of the inverters with 1 min time step in kWh per minute measured between 2019 and 2020. The capacity factor is therefore calculated by dividing the energy produced every minute by the installed power capacity and multiplying by 60 min/h. The hourly capacity factor is calculated summing the energy produced every minute and dividing by the installed power capacity. The system losses are 10 %. Fig. 3 shows the yearly normalized PV plant production profile in 2019 that has been measured. No data is missing in 2019. There was a case of a capacity factor exceeding 1 and preceded by zeros, indicating that this value represents energy produced in previous hours but not recorded. In such cases, the value exceeding 1 has been redistributed proportionally to the previous hours, using Renewables.ninja MERRA2 as a reference.

2.3.3. PV plant set-up and measurements in Utrecht, Netherlands (Cfb)

The data for Utrecht is collected from the open-source database presented in Visser et al. [51]. The database holds PV power measurements for 175 residential PV systems, which are rooftop mounted, over the period 2014–2017. For the purpose of this study one system with ID002 was selected. The selection is based on the high data availability of the PV system over the entire period, as well as due to the orientation of the PV system, which is more or less optimal with a tilt and azimuth angle of 30° and 170° (south), respectively. The PV system features

monocrystalline panels with an efficiency of approximately 15 % at STC. The system has an installed capacity of the 1.9 kWp, and an inverter capacity of 2.0 kWp, with an efficiency of about 97 %. More specific details on the PV system characteristics are confidential. Power measurements are collected on the AC side of the inverter through a data logger that records instantaneous power values at 0.5 Hz (approximately one power value is recorded per 2 s) [51]. The open-source dataset presented in Visser et al. holds filtered PV power measurements with a 1-min resolution, which are constructed considering the average of the registered power values. In this study, the main assessment considers the 1-min filtered power values, Figs. 3 and 7 are created using unfiltered 2 s data. From the 1-min time series, 8.6 % of data is missing. Missing values result from disconnection or a power outage of the data logger and/or the remote or originate from the data filtering process. This is explained in more detail in Visser et al. [51].

2.3.4. PV plant set-up and measurements in Almería, Spain (BWh)

The grid-connected photovoltaic power plant consists of a total of 9072 monocrystalline panels, mounted on a fixed support in the province of Almería, Spain, with a tilt angle of 22° and an azimuth of –2°. The installed solar panels are bifacial monocrystalline Longi (Hi-MO4 LR4-72HBD-440M) with an efficiency of 20.2 % at STC. They are connected to a Freesum inverter (Power Electronics), commercial reference FS3670KH000015, with an efficiency of 98.45 %. Each module has a power of 440 W, resulting in a total installed capacity of 3992 kWp, occupying a net area of 54,000 m². Performance and energy output measurements, both on the AC and DC sides, have been conducted using the OpenZmeter device [53], an open-source system for smart energy metering and power quality analysis. The OpenZmeter device is designed to comply with international standards such as IEC 61000-4-30 and EN 50160. OpenZmeter measures voltage in single or three-phase systems with an accuracy of up to 0.1 %, including DC systems. It supports standard frequencies of 50/60 Hz and can measure with a resolution of up to 10 mHz. Current measurement is determined by the selected external probe, including options like current transformers, Hall Effect sensors, and Rogowski coils. These probes allow for virtually unlimited current values, provided they comply with permitted input

levels. OpenZmeter is configured to store data in an internal circular database with different aggregation periods. It stores current and voltage data for 120 days with a sampling rate of 3 s and 1 min, respectively. Additionally, it stores aggregated data for 360 days with periods of 10 min and 1 h for current and voltage, and 15 min and 1 h for power measurements. In this installation, 4000A Rogowski coils and 40A current transformers were used for each of the strings. Measurements were taken in AC, and current, voltage, and power values from the inverter were recorded in parallel via Modbus communication. The inverter comprises 6 generation modules, with a total of 112 current measurements, one for each string, and 14 DC voltage measurements in each of the aggregation boxes. The analysed data consists of energy produced by the photovoltaic panels, recorded at various aggregation periods. Power production was calculated by summing the energies from lower aggregation levels. For example, hourly production was obtained by summing the four 15-min intervals for each phase. During data collection, there were recorded information losses due to communication issues, protection trips in different string lines, as well as technical maintenance and breakdowns. For instance, on September 2nd, a major inverter failure caused the plant to shut down. After maintenance, the plant was restored but with only 5 operational stages of the inverter, as one stage failed and needed replacement. During this period, the system operated at 80 % capacity until the failed module was replaced on September 14th.

2.4. PV-plant power time series simulation

The simulated PV-plant power time series are generated using open-source tools commonly used: Renewables.ninja [39], CorRES [54] and PVGIS [31]. These tools utilize different open-source dataset such as MERRA2, SARAH, SARAH2 and ERA5. MERRA2 [55] (Modern Era Retrospective-Analysis for Research and Application) is a global atmospheric reanalysis dataset that uses advanced data assimilation techniques and numerical models to combine satellite and ground-based observation. The resolution is 0.625° by 0.5°. SARAH and SARAH2 [56] (Surface Solar Radiation Data Set Heliostat) are satellite-based dataset derived from the observations of the geostationary Meteostat satellites. It has a higher resolution of 0.05° by 0.05°. ERA-5 [57] (European Reanalysis) is a global atmospheric reanalysis produced by the European center for medium-range weather forecasts (ECMWF). The spatial resolution is approximately 31 km. In the simulation tools considered, each dataset covers a limited range of years. In the PVGIS tool (Photovoltaic Geographical Information System), the SARAH dataset does not include years beyond 2016 (2015 in Renewables.ninja). Additionally, only Renewables.ninja and MERRA2 cover the year 2023. Both Renewables.ninja and Correlations in Renewable Energy Sources (CorRES) use the PVLib library to calculate the solar PV power output from the reanalysis data mostly based on [58]. PVGIS developed their own method to calculate the power profile. It is important to note that the PV power time series generated by different tools can be updated over time. In this study, it was observed that the original time series for Forlì, downloaded from Renewable.ninja and CorRES in July 2022, differed from those downloaded in September 2024. The version 5.2 of PVGIS was used at the time of the publication. Some of the simulated time series (i.e. Renewables.ninja SARAH in Forlì and Utrecht 2014) contained missing (zero) data points that were replaced by values from Renewables.ninja MERRA2.

To extract the hourly time series, both the PVGIS and Renewables.ninja APIs were used. To compare the different tools and datasets on the same basis, and be consistent with the experimental plant features, the same simulation set-up was applied for each run. Thus, in all cases, the system losses are set to the one measured on-site, and the tilt, azimuth and GPS coordinates are the same ones as the different experimental plants. The type of solar panels, inverter and the parametrisation used in the different tools can however hardly be changed. The default PV-panel technology used in Renewables.ninja and CorRES are based on

crystalline silicon (c-Si) solar cell, while PVGIS leaves the choice between c-Si, Cadmium telluride (CdTe) and copper indium gallium selenide solar cell (CIS) technologies. The PV-panel technology common to most of the experimental plants and all the tools is the c-Si solar cells. Therefore, this is the one chosen to construct the solar PV power time series. Finally, some modelling options are specific to the tool being used. For example, PVGIS allows the extraction of differentiated hourly time series through the API, providing differentiation between building-integrated and free-standing PV plants. The building-integration option for rooftop PV systems accounts for reduced efficiency due to higher temperatures in systems where ventilation is limited. This level of detail is not available in Renewables.ninja and CorRES. Furthermore, the simulation of bifacial panels is not supported in any of the tools considered. In this study, when possible, we use the simulation settings that most accurately reflect the characteristics of the experimental plant. The different combination and generated power profiles have been presented in Fig. 1 and the set-up of the different simulation and experimental plants are summarized in Table 2.

2.5. Comparison between simulated and measured PV power time series

The measured and simulated time series are compared using the following annual metrics: yearly average capacity factor differences (CF_{diff}), the Mean Absolute Error (MAE), and the Root Mean Square Error (RMSE).

The annual average capacity factor difference is calculated using Equation (1):

$$CF_{diff} = \frac{\sum_{i=1}^n CF_i^{sim}}{n} - \frac{\sum_{i=1}^n CF_i^{meas}}{n} \quad (1)$$

Where CF_i^{sim} is the simulated capacitor factor per period i (1 h), CF_i^{meas} the measured capacity factor at the experimental plant per period i , and n is the number of hours simulated and measured per year.

The yearly MAE is calculated using Equation (2):

$$MAE = \frac{\sum_{i=1}^n |CF_i^{sim} - CF_i^{meas}|}{n} \quad (2)$$

The yearly RMSE is calculated according to Equation (3):

$$RMSE = \sqrt{\frac{\sum_{i=1}^n (CF_i^{sim} - CF_i^{meas})^2}{n}} \quad (3)$$

2.6. Fuel plant set-up and techno-economic assessment model

The idea of this study is to use an e-fuel plant techno-economic assessment method that is one of the most commonly used in the literature. Therefore, this study uses a linear programming model that minimizes investment and operation costs for storage, power supply, and fuel production under constraints. The model used for this study, is an open-source model [47] used and presented in Refs. [6,60], and [61]. This type of optimization model is state-of-the-art for e-fuel plant techno-economic assessment and similar to the approach used in Refs. [17,22,30,62] among others. Linear programming models (and in some cases mixed integer linear programming models) have the advantage to be fast solving and relatively easy to implement which explains their relative popularity in the research community. However, these models have the limitation to use only one weather year as input assuming perfect foresight, thus not addressing power profiles uncertainties and multi-year variations. Still, the objective of this study is not to assess the relevance of using a method or another but to study the influence of using simulated power data or measured ones when applying this widely used method.

The power supply only consists in solar PV and the studied system is off-grid (islanded). It is assumed that the fuel producer owns all the production facilities that include a desalination plant, hydrogen and

Table 2

Set-up of the different PV power experimental plants and PV simulation tools.

| | Experimental PV plant | | | | Simulation tools | | |
|--|------------------------|-------------------|--------------------------|------------------------|--|------------------|-------------------------------|
| | Forlì, Italy | Turin, Italy | Utrecht, The Netherlands | Almería, Spain | Renewable ninja | PVGIS | CorRES |
| Available years | 2014–2015 ^a | 2019–2020 | 2014–2017 | 2023 ^b | Set identical to the experimental PV plant | | |
| Latitude | 44.223 | 45.065 | 51.970 ^c | 36.931 | | | |
| Longitude | 12.041 | 7.659 | 5.329 ^c | -2.472 | | | |
| Tilt ^d | 30° | 26° | 30° | 22° | | | |
| Azimuth ^d | 180° ^e | 206° ^e | 170° ^e | 178° ^e | | | |
| System loss | 5 % | 10 % ^f | 5 % | 9.75 % | | | |
| Building integration | Yes | Yes | Yes | No | Not in option | Same as PV plant | Not in option |
| Installed peak capacity (kWp) | 2.16 | 604.6 kWp | 1.90 kWp | 3992 kWp | 1 kWp | 1 kWp | 1 kWp |
| Inverter nominal capacity (kW, inlet/outlet) | 3.12/3.00 | 635 ^g | 2.0 | 3.8 MVA/3.67 MVA | Information not required | | |
| Inverter model | Power One Aurora 3.0 | Sunny Tripower | Confidential | Freesun FS3670KH000015 | Inverter model from [59] | Not specified | ABB-MICRO-0-25-I-OUTD-US-208V |
| Module manufacturer | CNPV | Benq | Confidential | Longi | PV panel model from [58] | Not specified | Canadian solar |
| Module model | CNPV-240P | SunForte PM096B00 | Confidential | LR4-72HBD-440M | PV panel model from [58] | Not specified | CS5P-220M |
| PV cell technology | Poli c-Si | Mono c-Si | Mono c-Si | Mono c-Si ^h | Poli c-Si | Poli c-Si | Poli c-Si |

^a Only partially.^b Year available only in Renewable ninja.^c Midpoint of the area reported in Visser et al. [51], values are based on system with ID002.^d In all cases there is no tracking system.^e Respectively 0°, 26°, -10° and -2° on the PVGIS website.^f Estimated.^g Multiple inverters.^h Bifacial PV panels.

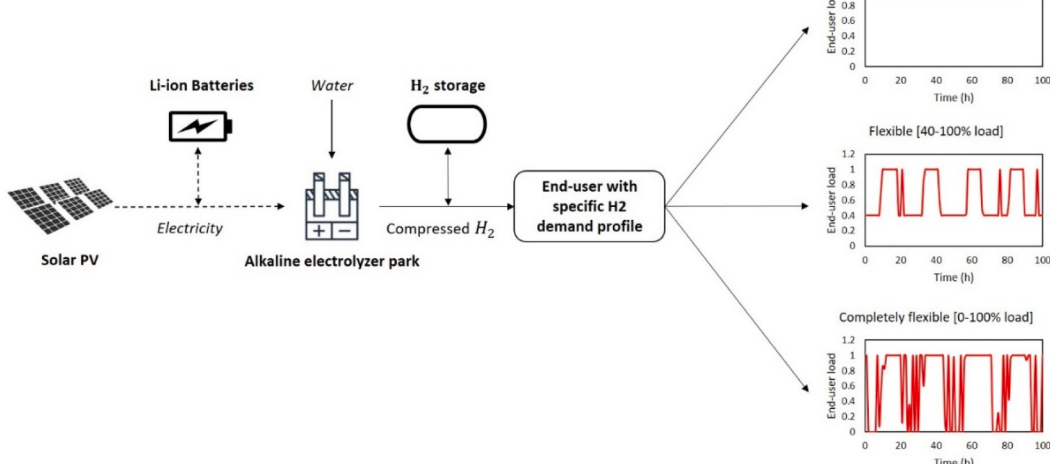
battery storages (if necessary), an electrolyser park, and a hydrogen end-user. Three different hydrogen end-user profiles are investigated in the study: “non-flexible”, “flexible” or “completely flexible”. In this work, a non-flexible end-user needs a constant supply of hydrogen all year round to ensure full load operation. A completely flexible end-user can handle a variable hydrogen supply and shut down its operation if required. A flexible user can handle a variable hydrogen supply but must operate above a given minimal load and is therefore not allowed to rapidly shutdown completely. The end-user taken for example in this study is an ammonia plant (Haber-Bosch) and its air separation unit (ASU). However, the conclusions of the study would remain valid for other end-users with similar hydrogen demand profiles. Based on [6], the minimal load of the flexible user (ammonia plant) is 40 % of the nominal capacity.

A simplified flowchart of the e-fuel plant set-up is presented in Fig. 4, where the three consumption profiles under investigation are schematically shown.

The mathematical formulation of the linear model is taken from Campion et al. [6]. The objective function minimizes the total system costs and is written as:

$$\text{Min}_{x_{u,t}, c_u} = \sum_u (I_u * A_u + F_u) * c_u + \sum_{u,t} (V_u + P_{u,t}) * x_{u,t}$$

Where t is the set of time (hours of the year) and u is the set of units composing the e-fuel plant. The variable (positive) are $x_{u,t}$, the output flow of mass or energy from unit u at time t and c_u , the installed capacity of unit u. $P_{u,t}$ is the hourly price of the output from unit u at time t. F_u and

**Fig. 4.** E-fuel plant set-up.

V_u are the fixed and variable O&M costs of unit u. I_u is the investment expenditure of unit u and A_u the annuity factor, in this study equal to the capital recovery factor using a discount rate of 8 %.

The driving constraint is the yearly fuel production target D_u that must be satisfied, $MinD$ being the subset of units required to produce the end-fuel (for example an ammonia plant):

$$\sum_t x_{u,t} = D_u \quad \forall_{u \in MinD}$$

Due to their limited effect on the results [6], ramping constraints have been excluded. Still, the different units of the system are constrained to operate between their minimal load L_u^{min} and their installed capacity at all time:

$$c_u * L_u^{min} \leq x_{u,t} \leq c_u \quad \forall_{u,t}$$

Then, the electricity produced by a unit u belonging to the subset of intermittent power units ψ (here the solar PV plant) is equal to the installed power capacity multiplied by the normalized power profile $PP_{u,t}$ of the unit u at time t. Values of $PP_{u,t}$ are then between 0 and 1.

$$PP_{u,t} * c_u = x_{u,t} \quad \forall_{u \in \psi, t}$$

The following constraint is enforced to ensure that chemicals reaction mass balances are respected. P_i is the subset of units synthesizing a product using a reactant coming from a unit belonging to the subset R_i .

$$x_{P_i,t} = x_{R_i,t} * PR_{P_i} \quad \forall_{i,t}$$

The balance of the different storage systems is ensured by the following constraint where T_j is the subsets of units behaving like a tank, In_j the subset of units used to charge a tank, and Out_j the subset of units used to discharge a tank. ρ_u^in and ρ_u^out are the charging and discharging efficiencies of unit u. At $t = 0$, the tanks are empty but the plant can operate without minimal load constraints during 10 days (240 h) to leave time for the tanks to charge.

$$x_{u \in T_j, t} = x_{u \in T_j, t-1} + \rho_{u \in In_j}^in * x_{u \in In_j, t} - \rho_{u \in Out_j}^out * x_{u \in Out_j, t} \quad \forall_{j, t > 1}$$

Finally additional balance constraints are added to ensure that the power and hydrogen balances are respected at all time (one constraint per commodity). $Cons_u$ is the consumption (when negative) or the production (when positive) of electricity or hydrogen of a unit u.

$$\sum_u Cons_u * x_{u,t} = 0 \quad \forall_t$$

The techno-economic input data used in the model are presented in Table 3.

Since, the price of water supply is usually negligible compared to the other expenses, it is neglected to simplify the case study [6,17].

3. Results and discussion

This section is divided in three subsections. The first one presents the difference between the simulated and measured time series for the different data set and simulation tools used. The second analyses the

error propagation from the time series data to an e-fuel plant techno-economic assessment and compares the time series induced error with the uncertainty of other parameters such as electrolyser and solar PV costs, electrolyser efficiency, solar PV costs, and weighed average cost of capital (WACC).

3.1. Comparison between simulated and measured PV power time series

Fig. 5 shows the correlation between the measured (abscissa) and simulated (ordinate) time series for the site of Forlì, Italy, using normalized data from various models. Each subplot corresponds to a different simulation dataset (e.g., RN-MERRA2, RN-SARAH), and the color gradient illustrates the density of data points through Kernel Density Estimation (KDE). The red/yellow regions represent high-density areas where simulated values strongly overlap, while the blue areas indicate lower densities. The red points represent the measured values, illustrating the ideal fit. If the high-density areas are located above the red line, it indicates an overestimation of the simulated data, while points below the line suggest underestimation. The proximity of the data to this line indicates how well each model matches the real-world observations. The same comparison for the other sites is available online by running the PV time series analysis tool from the public repository [46].

The RN-MERRA2 (the power profile generated with Renewables.ninja using the MERRA2 dataset) simulation shows the strongest overestimation, with most of the hourly data points concentrated above the measured data points (red dots), indicating that the simulated values are consistently higher than the observed values. MERRA2, SARAH, SARAH2 dataset usually overestimate the solar power production and this result is consistent with the literature [40,45,66]. Simulation based on the ERA-5 dataset, seems however to have a better correlation with the measured power profile. A similar behaviour has been observed in Utrecht for the years considered; in this case, the ERA-5 dataset also shows outputs that are more closely aligned to the measured data. In the case of data from Turin, all tools and datasets, including ERA-5, show capacity factors overestimation, particularly for the year 2020.

Fig. 6 shows the yearly duration curve of the capacity factors for the measured and simulated time series for different years and locations. In this regard, it is possible to analyze more precisely when the error occurs.

Similarly to the previous graph, Fig. 6 confirms that RN-MERRA2 systematically overestimates the solar potential across all hourly capacity factors, for all years and sites, except Almería. In Almería, the PV panels from the measurement station are bifacial and higher capacity factors are expected compared to the mono-facial panels modeled in Renewables.ninja, which does not support bifacial panel simulation. Despite this, the simulated capacity factors are higher than the measured values during low-capacity factor periods, suggesting that RN-MERRA2 still overestimates solar resources in Almería, particularly during those hours. It is also evident that PV power calculation tools using the same dataset produce significantly different power production estimates, highlighting the importance of the methods used for power estimation,

Table 3

Main techno-economic parameters used in the model.

| | CAPEX | Fixed O&M | Electrical consumption | Flexibility | Lifetime |
|---|--|--------------------------------|--|------------------------------------|---------------|
| Electrolyser AEC [6] | 56.5 k€/(kg _{H2} /h) ^a | 2 % CAPEX | 51.5 kWh/kg _{H2} | [0–100 %] | 25 years |
| Solar PV [6] | 550 €/kWp | 9.1 €/kW/y | – | – | 35 years |
| Hydrogen storage (underground pipes) [63] | 461 €/kg _{H2} | 1 €/kg _{H2} /y | Compression 30–100 bars 0.94 kWh/kg _{H2} | Max discharge level of 91 % | 50 years |
| Batteries | 362 €/kWh [64] | 5.1 €/kWh [7] | 0.09 kWh/kWh _{stored} [65] | Max discharge level of 80 % | 20 years [65] |
| H2 end user | | | | | |
| Ammonia plant (incl. ASU) [6] | 4192 €/(kg _{NH3} /h) | 436 €/(kg _{NH3} /h)/y | 0.38 kWh/kg _{NH3} | [0–100 %] [40–100 %] [100 %] | 25 years |

^a Includes stack replacement cost every 10 years using stack net present value.

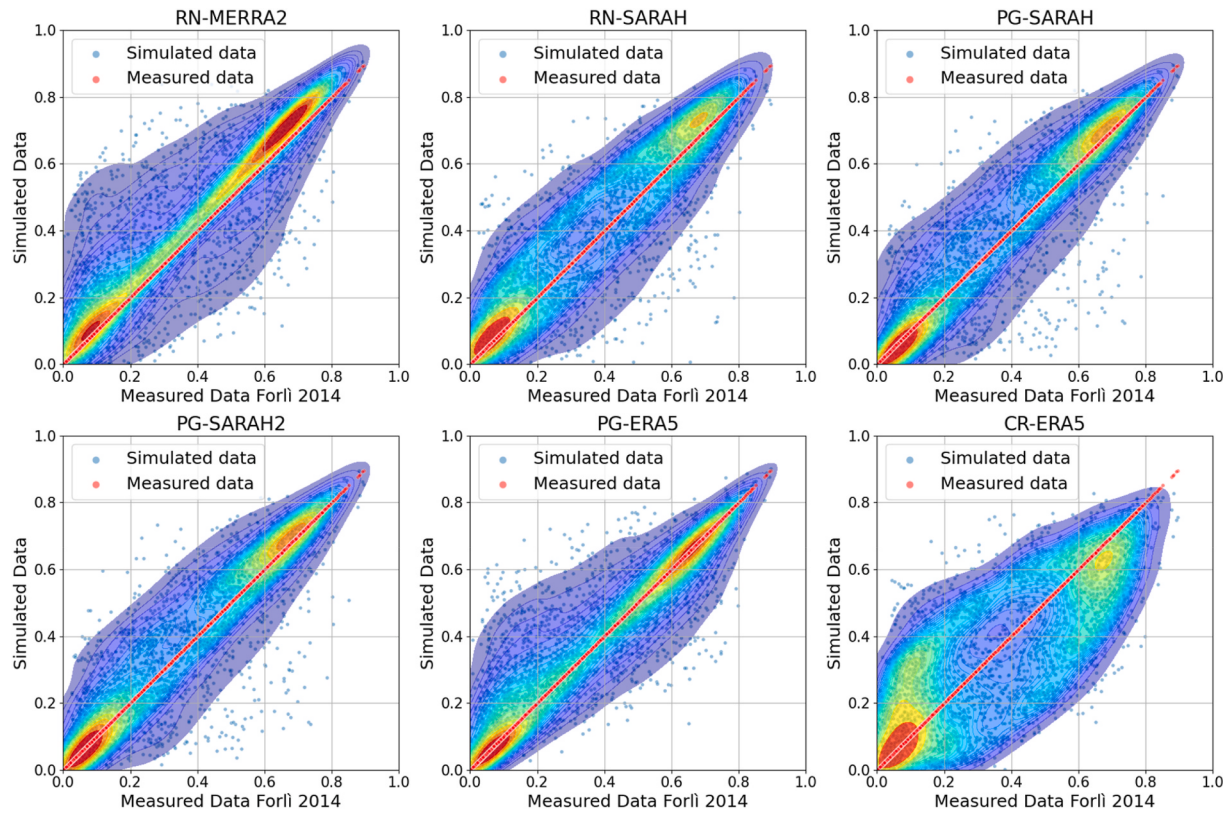


Fig. 5. Simulated and measured time series correlation in Forlì 2014–2015.

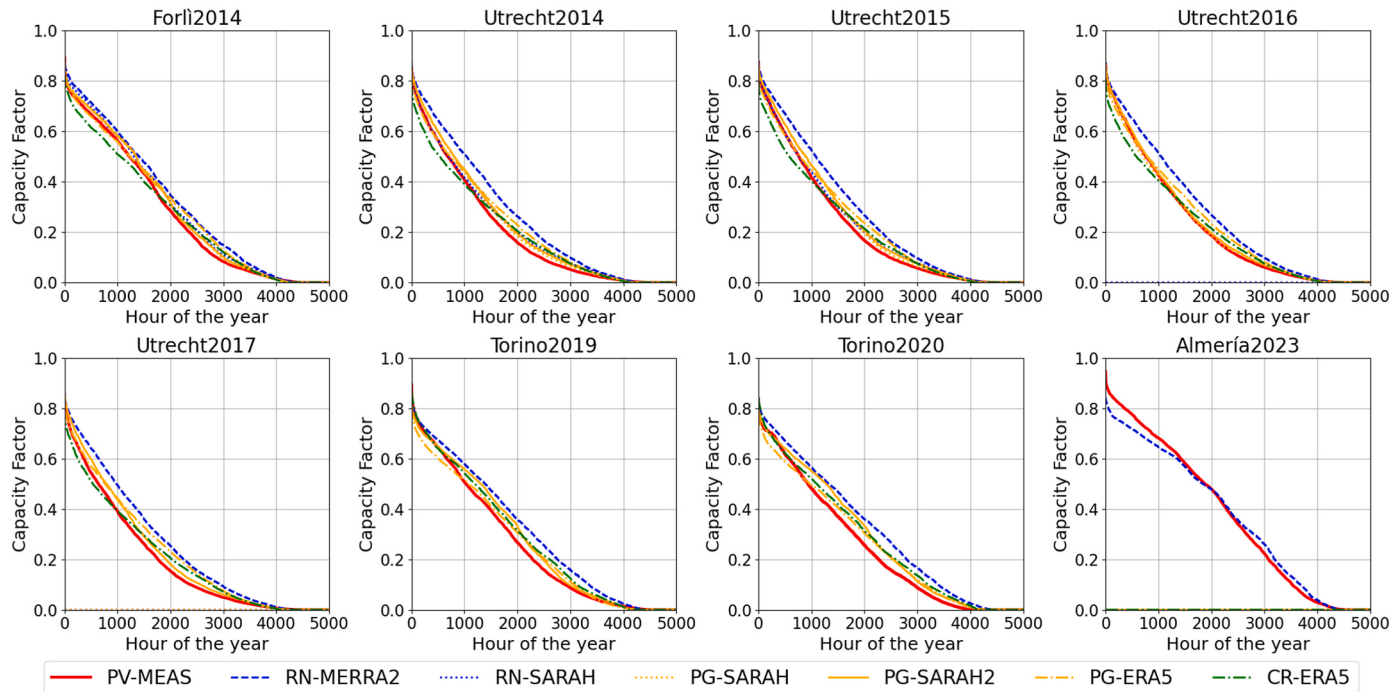


Fig. 6. Duration curves comparing measured (PV-MEAS) with simulated data.

such as accounting for losses due to high temperatures. For instance, PVGIS offers the option to model either building-integrated or free-standing systems, which may explain why its results are more closely aligned with the measured data. Another key observation is that the discrepancy between simulated and measured capacity factors is

consistently larger for low-capacity factors (between 0.4 and 0.05), typically occurring on cloudy days. Among the models, PG-SARAH2 and PG-SARAH are the closest to the measured values during these low-capacity factor periods, whereas RN-MERRA2 and PG-ERA5 tend to estimate higher capacity factors in this range. Overall, the significant

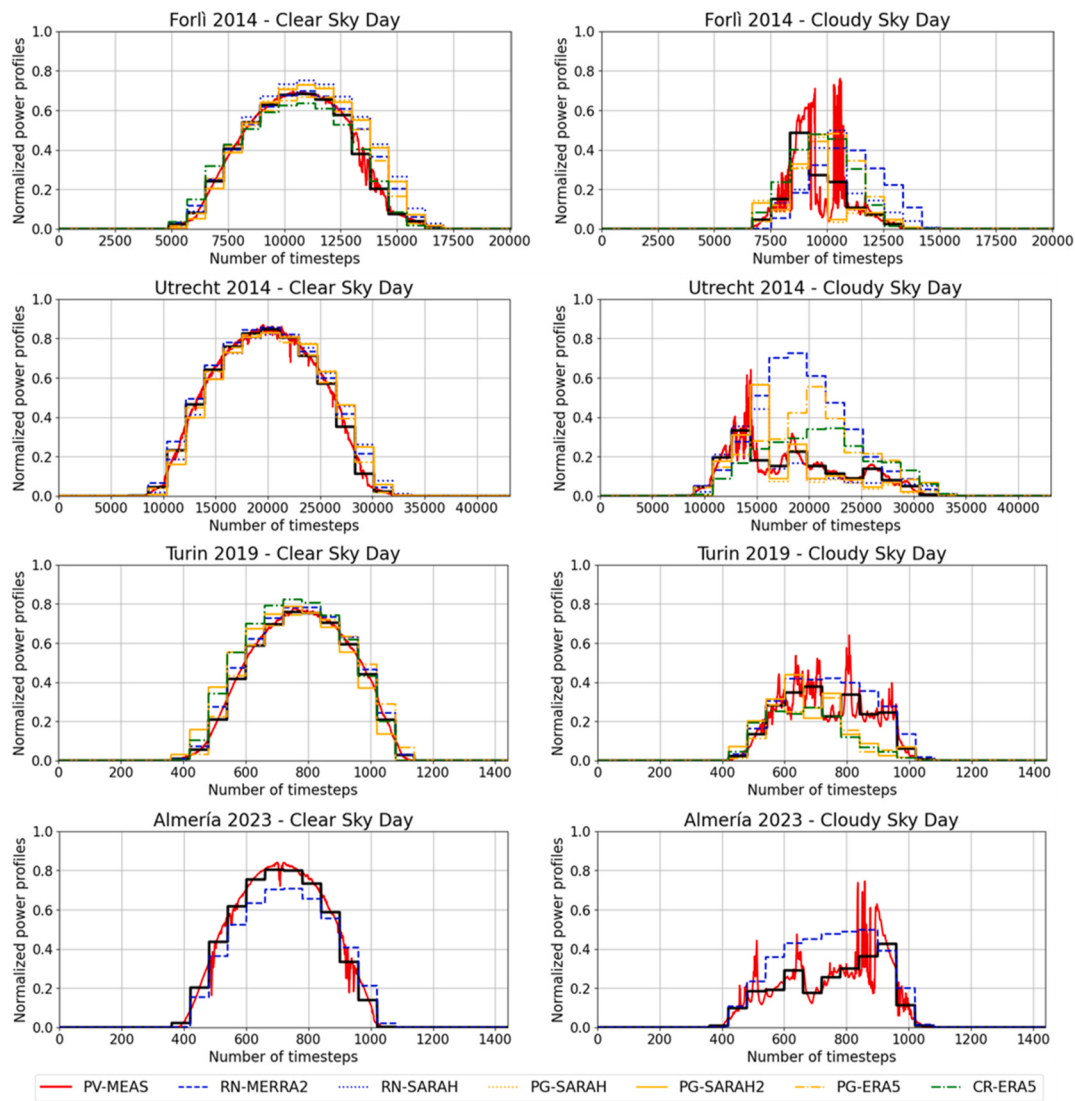


Fig. 7. Comparison of simulated and measured time series based on high-resolution data.

differences between measured and simulated power profiles may stem from the challenges in accurately estimating hourly average capacity factors during cloudy conditions.

Fig. 7 shows high resolution data for both a cloudy and a clear-sky day. By analyzing the figure, it is possible to provide an interpretation for the larger error observed, particularly in relation to the impact of cloud cover on the simulations.

During a cloudy day, with frequent alternation between high and low irradiance episodes (right side of Fig. 7), the calculation of the hourly capacity factor average differs significantly between the measured and simulated values. As noted in the PVGIS documentation, the hourly satellite data points are not derived from an average of multiple observations but from a single data point taken at a “random” time within the hour. If this point is captured during a cloudy period, the hourly capacity factor will be low, whereas if it is recorded during a brief sunny period, the hourly capacity factor will be high, even if the measured hourly average capacity is low. This explains why, during the time steps between 9000 and 11,000 in Forlì, the measured average power (black line) is low, while all the simulated time series overestimate the available power. It also explains the significant differences in power production estimates from different tools within the same cloudy hour, as each tool may select its data point at a different time within that hour. Inaccurate cloud modelling, as notably mentioned by Ref. [40] for the

MERRA-2 dataset, may also explain the large power production values observed during cloudy episodes, particularly with the ERA-5 and MERRA-2 datasets. This aligns with the findings of [67], who reported that MERRA-2 (and ERA-Interim) sometimes predicts clear-sky conditions when the sky is actually cloudy.

On a generally clear-sky day (left side of Fig. 7), the simulated time series align much more closely with the measured hourly average. However, the “single data point measurement” approach may still explain some differences between the measured and simulated time series. If the data point is taken at the beginning of the hour, the hourly capacity factor may be overestimated in the afternoon and underestimated in the morning, as observed with the RN-MERRA2 time series. While, if the point is taken at the end of each hour, the capacity factor could be overestimated in the morning and underestimated in the afternoon. Ideally, this assumption could be tested by checking the exact time of the satellite measurement point and comparing it with ground-based measurements. However, this information is not available from the tools assessed. It is important to note that these patterns remain consistent across different sites and years.

The graphs in Fig. 8 present the errors in CF values between measured data and the estimations from selected simulation tools across various years and locations. The first graph shows the annual average CF differences (CF_{diff}), with positive values indicating overestimations by

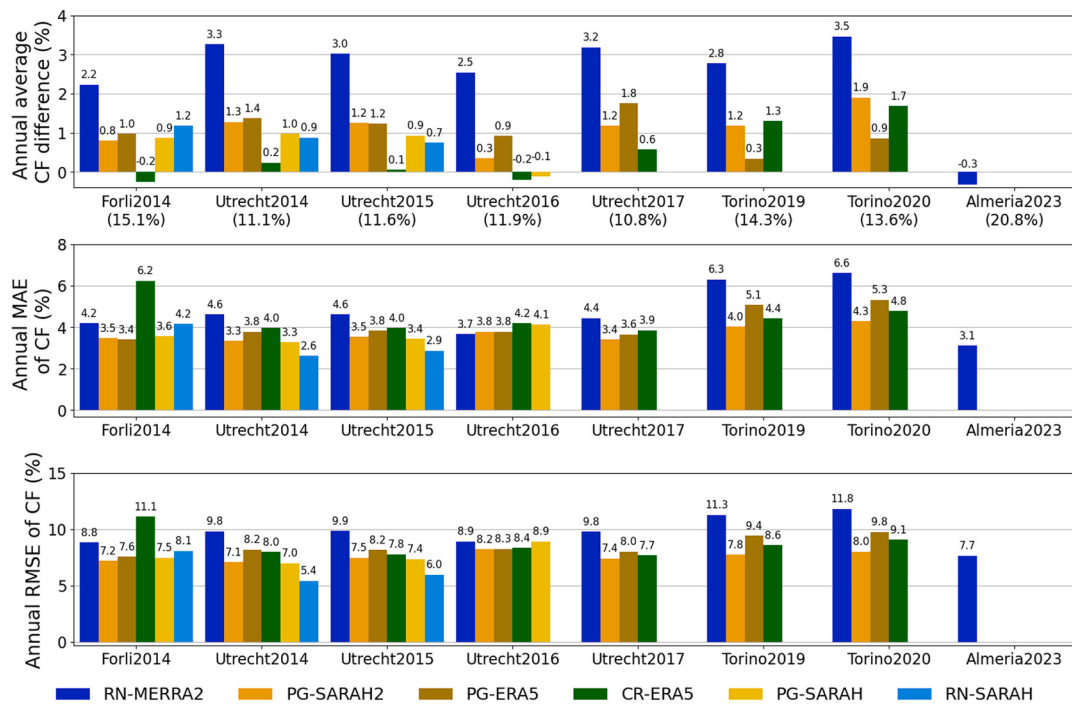


Fig. 8. Yearly error measurement between simulated and measured times series across various locations and years, with a focus on three metrics: the annual CF difference (CF_{diff}), the mean absolute error (MAE), and the root mean squared error (RMSE).

the simulation tools. The average measured CF for each location and year is provided in parentheses beneath the location name, with higher average CF for the bifacial plant in Almería and lower for the plant in the Netherlands. The second graph shows the mean absolute error, representing the average magnitude of errors between the measured data and the simulation tools, with lower values indicating better accuracy. The third graph illustrates the root mean squared error, which penalizes larger errors more heavily by squaring the differences.

The first graph shows that most of the simulation tools have a positive CF_{diff}, indicating that they tend to overestimate the CF, except for CR-ERA5 in Forlì and Utrecht 2016 and PG-SARAH in Utrecht 2016. The graph confirms the high overestimations of RN-MERRA2 across all locations, and the exception for Almería 2023, due to the bifacial plant that do not allow direct comparison. CorRES, using ERA5 dataset tends to have smaller deviations from the measured data, except for a significant overestimation in Torino (between 1.3 % and 1.9 %). Other tools, like PG-SARAH2, PG-ERA5 and PG-SARAH, also show moderate overestimations. The same dataset (SARAH) with the two different tools Renewables.ninja and PVGIS gives different results, showing that the post-processing of the weather dataset also has a significant influence on the results.

The differences between MAE and RMSE graphs are relatively small, suggesting that there are not many extreme outliers or large deviations that would significantly inflate the RMSE values. RN-MERRA2 show higher errors across most locations, while CR-ERA5 shows particularly high MAE in Forlì 2014 (6.2 %). PG-SARAH2, PG-ERA5 and RN-SARAH show consistent performance with MAE values ranging from 2.6 % to 4.2 %, demonstrating lower error magnitudes across all locations.

The plants in Utrecht and Turin allow comparisons between different years: in both locations, during the year with highest average CF, the simulated time series show lower CF_{diff}. In the PV plant in Turin in the year 2019, with an average capacity factor of 14.3 %, the CF_{diff} is in a range between 0.3 % and 2.8 %, with a better performance of the ERA5 dataset and PVGIS tool. While in 2020, with an average capacity factor of 13.6 %, the CF_{diff} ranges from 0.9 % to 3.5 %. In Utrecht 2016 with

high average CF, the CF_{diff} spans from -0.2 % to 2.5 %, while in 2017, with low average CF, it ranges from 0.6 % to 3.2 %. This behaviour supports the hypothesis that more cloudy days can lead to greater uncertainties.

3.2. Error propagation to the e-fuel techno-economic assessment

As presented in the methods section, a techno-economic assessment of an e-fuel plant is performed using both simulated and measured time series data. The model used is a state-of-the-art linear cost optimization model minimising both investments and plant operations [6,47]. Various hydrogen end-user consumption profiles are analysed: non-flexible, flexible, and completely flexible. In this case, the hydrogen end-user is an ammonia plant. A non-flexible profile means that the ammonia plant operates at full load continuously, while the flexible profile allows operation between 40 % and 100 % load, and the completely flexible profile permits operation between 0 % and 100 % load. The yearly ammonia production target is set to 100 ktonnes of ammonia, requiring around 18.1 ktonnes of green hydrogen as input. Fig. 9 shows the relative error in levelized cost of fuel (LCOF)—specifically, in this case, the levelized cost of ammonia (LCOA)—across different sites and years when simulated PV power time series are used instead of measured data for the techno-economic assessment of the e-fuel plant.

It is observed that all tools and datasets consistently underestimate the LCOF for all sites and all years. In general, the LCOF error decreases for hydrogen end-users that are more flexible. None of the tools appears to consistently outperform the others across all sites and years; however, RN-MERRA2 usually gives the largest LCOF when the hydrogen end-user is completely flexible. In Almería, the LCOF error is consistently low, primarily because the bifacial PV panels at the measurement station are more efficient than the monofacial panels modeled in the simulations. Measured data for monofacial PV panels from the Almería site were not available at the time of the study but will be shared in the public repository associated with this study [46] once they become available.

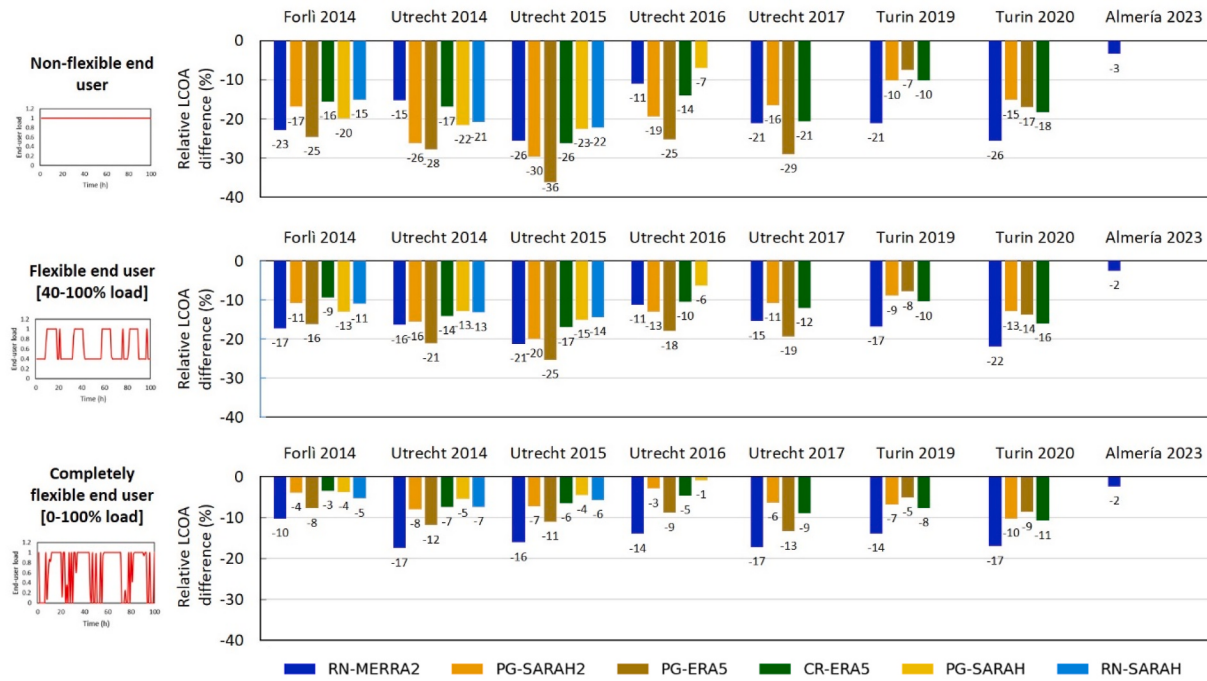


Fig. 9. Relative error in LCOF from using simulated instead of measured PV power time series for different sites, years, reanalysis dataset and simulation tools.

3.2.1. Explanation of the error propagation with the study case of Forlì

This section focuses on the study case of Forlì in the year 2014–2015 (from 03 to 10–2014 to 30-09-2015) to explain the error propagation from PV power time series to fuel production costs estimates. Most of the interpretations made in this section can be extrapolated to other sites with similar characteristics. Fig. 10 provides a detailed cost breakdown and the associated LCOF for an optimized e-fuel plant system in Forlì.

It can be observed that the underestimation of LCOF when using

simulated PV power time series is associated with underestimated costs for the PV plant, electrolyzer, intermediate hydrogen storage, and, to a lesser extent, the battery system. This occurs because the overestimation of solar resources in all the simulated time series leads to an undersized e-fuel production system compared to the one sized using measured PV power profiles, as shown in Table 4.

In Forlì, the cost underestimation is between 9.3 and 17.3 % for flexible hydrogen end-users and between 24.6 % and 15.1 % for non-

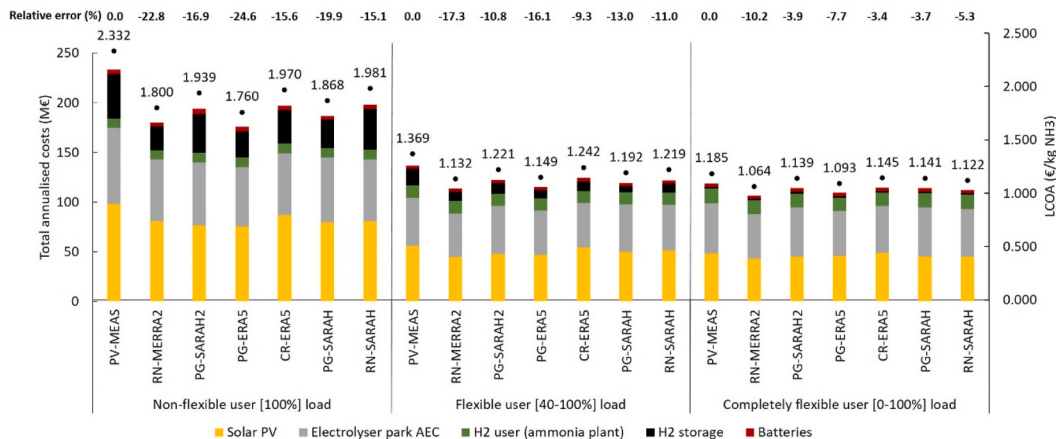


Fig. 10. Cost breakdown, LCOF and relative difference with the PV-MEAS input time series in Forlì 2014–2015 (Italy).

Table 4

Optimal installed capacities in Forlì 2014–2015 depending on the PV power profile time series.

| Fuel plant unit | Installed capacities for a specific PV power profile with a flexible end-user [40–100 %] load | | | | | | |
|---|---|-----------|-----------|---------|---------|----------|----------|
| | PV-MEAS | RN-MERRA2 | PG-SARAH2 | PG-ERA5 | CR-ERA5 | PG-SARAH | RN-SARAH |
| Electrolyser AEC (t_{H2}/h) | 7.6 | 6.9 | 7.5 | 7.0 | 6.9 | 7.4 | 7.1 |
| H2 storage (t_{H2}) | 433.3 | 236.4 | 273.1 | 205.7 | 252.6 | 154.0 | 243.3 |
| Batteries (MWh) | 84.4 | 72.6 | 73.2 | 69.6 | 79.5 | 78.5 | 77.9 |
| Solar PV plant (MW) | 991.3 | 787.3 | 850.3 | 824.3 | 968.2 | 885.2 | 906.3 |
| Flexible ammonia plant (t_{NH3}, h) | 14.8 | 15.3 | 15.3 | 15.1 | 14.6 | 15.0 | 14.9 |

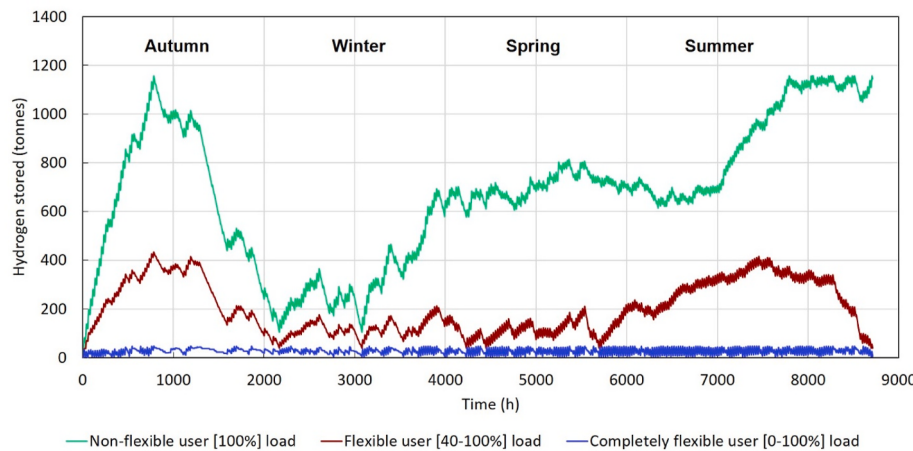


Fig. 11. Optimal intermediate hydrogen storage behaviour depending on the end-user flexibility in the site of Forlì using measured PV power data. First data point is 03-10-2014 and last 30-09-2015.

flexible hydrogen end-users. For a fully flexible end-user, the cost estimates error is reduced to $[-10.2, -3.4\%]$. Similarly to what Mathews et al. [45] observed, these differences are due to how the hydrogen storage is sized and operated. As shown in Fig. 11, when the hydrogen end-user must operate at full load all year, the storage is used in a seasonal configuration, requiring large investments in storage capacities but also electrolyser and PV plant capacities to produce enough hydrogen in summer to have it available in winter and produce the required amount of ammonia. In this case, the solar PV plant must be two times larger and the hydrogen storage six times larger compared with the flexible end-user. For a more flexible end-user, operating above 40 % load all year round, the storage is operated with shorter cycle and smaller capacities are required to satisfy the end-user hydrogen demand during winter. Finally, when the end-user is completely flexible, meaning that the ammonia (or methanol) plant would be able to be rapidly shut down on a regular basis, the hydrogen storage needed is much smaller and operates for daily cycles rather than seasonal storage. In this case, overestimating the solar resources has a lower influence on the LCOF estimates as the invested capacities for hydrogen storage (and subsequent electrolyser and PV plant oversizing) are limited.

Similar optimal hydrogen storage operation patterns are observed in the sites of Utrecht, Turin and Almería. In Almería, due to lower seasonal variability, the hydrogen storage size is reduced but is still operated as seasonal storage for non-flexible hydrogen end-users. E-fuel plants that combine wind and solar power or have access to grid back-up power typically observe storage operations limited to daily (or weekly) cycles [6]. For these types of systems, the error induced by PV power time series simulation should be reduced.

3.2.2. Comparison with the error of other uncertain parameters

Using simulated or measured solar PV data has clearly a significant impact on the LCOF estimates and optimal system design. However, when assessing power-to-X systems, a large variety of other techno-economic parameters are also uncertain and can influence the results. Comparing the influence of other parameters uncertainties with the ones inherent to simulated power time series gives an idea on where the focus is the most needed to obtain reliable data. Various studies performing sensitivities analysis on power-to-X systems [15,68–70] already identified that the most sensitive parameters to the costs estimates are the weighted average cost of capital (WACC) (or discount rate), the cost of the electrolyser and the cost of the renewable power supply. Considering a flexible hydrogen end-user ([40–100 %] load, which is a common practice in literature, the LCOF obtained in Forlì is 1132 €/t_{NH3} using RN-MERRA2 and 1369 €/t_{NH3} using PV-MEAS (+20.9 % compared to using RN-MERRA2). Fig. 12 shows the extent of parameter variation required to achieve a similar change in LCOF (LCOA). The simulated time series chosen for comparison is the default option from Renewables.ninja (RN-MERRA2) which one of the most popular options in the literature.

These results demonstrates that the error inherent to use simulated PV power profiles instead of measured ones is rather significant compared to the uncertainties of other parameters. Indeed, an overestimation of PV or AEC capex (and the associated opex increase) of 56 % is needed to have the same influence of using a measured profile instead of a simulated one. For comparison, the Danish Energy Agency (DEA) technology catalogue [71] gives an uncertainty range between -3.5% and $+7\%$ for utility scale PV plant capex (between 540 and 600

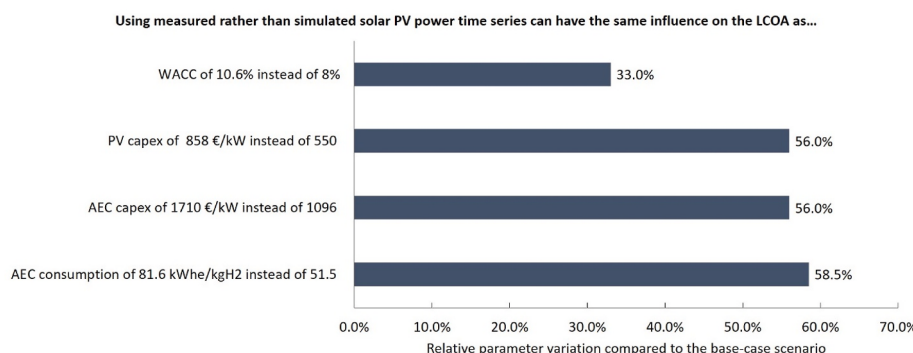


Fig. 12. Influence of using a measured PV power time series (PV-MEAS) rather than a simulated (RN-MERRA2) compared to other parameters variation for a flexible hydrogen end-user. Capex variations are associated with opex values as opex values are expressed in percentages of capex.

€/kW with 560 €/kW as benchmark value in 2020). The Irena reports that the 5th and 95th percentile of 2022 total installed cost for utility-scale PV plants ranges between 569 and 1878 USD/kW with a weighted average of 876 USD/kW so with maximum variations between −35 % and +114 % [72]. Regarding large scale electrolysis (AEC) plant Capex, the DEA technology catalogue reports min-max values between 400 and 800 €/kW [71] while Irena proposes a range between 437 and 875 €/kW [73] (excluding stack replacement costs). Using the measured time series instead of a simulated one has the same influence on the LCOF as difference of 614 €/kW in electrolyser capex which is actually higher than the min-max range proposed by DEA and Irena. Similarly [73], estimates AEC electrolysis system efficiencies between 50 and 82 kWh/kg_{H2} meaning that choosing the high-end electrical consumption value instead of the low-end one is equivalent to using a measured solar PV profile instead of a simulated one. The local WACC (or discount rate) in most countries usually varies between 5 and 9 % [15]. A 2.6 % absolute WACC difference is enough to reach the same effect as using a measured time series, meaning that the uncertainties related to the WACC are likely to have a greater or similar influence than the one related to PV time series quality. The uncertainties associated with factors like the PV or the electrolyser plants' lifetime, as well as other parameters that were found to have a limited impact on LCOF in prior analyses such as ammonia plant ramping rates [6], compressors costs [15], hydrogen storage costs [70], batteries costs [15], ammonia plant costs [70], appear to have a much lower importance compared to the inherent PV simulated power profile uncertainties.

3.3. Results summary and recommendations

Table 5 summarizes the key findings of this analysis, presenting a comparison between the PV power time series generated from simulations and those derived from measurements. It also compares the outcomes of the techno-economic assessment for e-fuel (e-ammonia)

production when using simulated or measured PV power time series as input. The table presents the result range obtained from all the different sites and years. However, the site of Almería was removed due to the limited number of simulations tools available for the year 2023 at the time of the publication. New data will be added on the public repository [46] when available.

A general observation is that, in most cases, the error propagation from the PV power time series to the LCOF estimates is quite significant, the effect being more pronounced for non-flexible hydrogen end-users. **Table 5** also shows that a relatively small error difference between the measured and simulated time series can be largely amplified when calculating the LCOF for the off-grid solar powered system analysed in this study. Accurately measuring the annual capacity factor does not necessarily guarantee a low error in estimating the LCOF. For example, in Utrecht 2016, with a non-flexible end user, CR-ERA5 provided the most accurate estimate of the annual capacity factor, with a CF_{diff} of −0.2 %. However, it ranked only third in estimating the LCOF, with an error of −14 %. The tools and datasets that are most accurate for LCOF estimation also tend to vary across different sites and years. In some cases, such as in Turin, PG-ERA5 consistently delivered the most accurate LCOF estimates for all hydrogen end-user consumption profiles in 2019, but this was not the case in 2020. Some of these observations can be attributed to how different simulations perform when estimating the capacity factor during cloudy or winter days. If the intermediate hydrogen storage is used seasonally or in monthly cycles, overestimating solar resources in winter can significantly influence storage investment decisions. This, in turn, leads to oversizing the related PV plant and electrolyser, thereby increasing the LCOF error. As shown in **Fig. 6**, which presents capacity factor duration curves, simulations that closely match the measured time series for lower capacity factors tend to deliver more accurate LCOF estimates. Based on these observations, it can be concluded that when hydrogen storage is used seasonally, accurately estimating the yearly average capacity factor is not the key factor for

Table 5
Results summary.

| Site description -Location -Years of measurements -Climate | Solar PV power time series comparison | | | E-fuel techno-economic assessment comparison | | | |
|--|--|---|---|---|--|--|---|
| | Values (%) with associated time series and year | | H ₂ end-user flexibility | H ₂ storage operation | LCOF differences ^a (%) | | |
| | Min | Max | | | Min | Max | |
| Forli, North Italy 2014–2015 Humid subtropical climate (Cfa), hot and humid summers, cool and damp winters | CF _{diff} CR-ERA5 MAE RMSE | −0.2 % 3.4 % 7.2 % 0.3 % | 2.2 % 6.2 % 11.1 % 3.5 % | Non flexible ^b Flexible ^c Fully flexible ^d Non flexible | Seasonal cycles Monthly cycles Daily cycles Seasonal cycles | −15.1 % −9.3 % −3.4 % −7.5 % | −24.6 % −17.3 % −10.2 % −25.6 % |
| Turin, North Italy 2019–2020 Humid subtropical climate (Cfa) | CF _{diff} PG-ERA5 (2019) MAE RMSE | 0.3 % 4.0 % 7.8 % PG-SARAH2 (2019) | 3.5 % 6.6 % 11.8 % RN-MERRA2 (2020) | Flexible Fully flexible | Monthly cycles Daily cycles | PG-ERA5 (2019) −7.8 % −5.1 % | RN-MERRA2 (2020) −21.9 % −21.9 % |
| Utrecht, The Netherlands 2014–2017 Temperate oceanic climate (Cfb), warm summer, cool winters, frequent clouds | CF _{diff} CR-ERA5 (2016) MAE RMSE | −0.2 % 2.6 % 5.4 % CR-ERA5 RN-SARAH (2014) | 3.3 % 4.6 % 9.9 % RN-MERRA2 (2014) | Non flexible Flexible Fully flexible | Seasonal cycles Seasonal cycles ^e Daily cycles | PG-SARAH (2016) −6.3 % −0.8 % | PG-ERA5 (2015) −25.3 % −17.5 % |
| | | | | | | PG-SARAH (2016) −25.3 % −17.5 % | RN-MERRA2 (2014) |

^a The relative LCOF difference is obtained using the measured time series as reference. Here, the hydrogen end-user is an ammonia plant.

^b Always full load operation.

^c Operation between 40 and 100 % load, no possibility to shut down the plant.

^d Operation between 0 and 100 % load.

^e Except when using the year 2015, where monthly cycles are optimal.

achieving reliable LCOF estimates and relying solely on this parameter for cost predictions is misleading. Instead, the accuracy of PV power profile simulations during cloudy and winter days plays a more critical role, as it strongly influences the optimal sizing of hydrogen storage and the overall plant configuration. Similar observations were also made by Ref. [45], which comforts the conclusions of the present analysis. These results apply to islanded (off-grid) fuel production systems. If a grid connection is available alongside the PV power supply, the error propagation to LCOF estimates from PV power simulations is likely to decrease. This is because the need for intermediate storage and system oversizing would be reduced [6]. For a completely flexible end-user, where hydrogen storage sizing has less impact on the LCOF, the performance of different simulation tools varies. As expected, RN-MERRA2 consistently underestimates the LCOF the most, which aligns with its poorer performance compared to other tools across CF_{diff}, MAE, and RMSE indicators.

In locations where measured data is unavailable, modellers can use various methods to mitigate the errors inherent in simulated time series. One approach is to assume higher PV system losses in the simulations, which can help lower the overall error in LCOF estimates. However, this method may still lead to undersized system designs, as simulated time series often fail to accurately represent non-clear sky conditions and winter days. Modelling the hydrogen end-user as a completely flexible off-taker and avoiding seasonal use of hydrogen storage can also help reduce the error propagation from PV power time series to LCOF estimates, although errors of up to 17.5 % may still occur in cloudy climates. Finally, simulating PV panels with lower performance than actual conditions (e.g., using monofacial instead of bifacial panels) could be another strategy to minimize LCOF errors. While these approaches, along with a critical evaluation of the LCOF estimates, may be adequate for modelling purposes, actual investment decisions and plant sizing should be based on high-quality, ground-measured PV power production data from locations near the proposed hydrogen production site. Developing open-access datasets that include validated PV generation data from various existing production sites would help stakeholders minimize the risk of project failure. For locations where no existing data is available, an alternative would be to set up a small-scale PV test bench (on the order of kilowatts) before deploying the electrolyser and other Power-to-X components. This would allow for experimental verification of the real renewable energy production potential.

4. Conclusion

This study has focused on assessing the impact of solar power profile simulation bias when leading techno-economic assessment of islanded e-fuels production systems. The study compares the effect of using PV power time series generated with standard open-source models using reanalysis data versus using experimental data in e-fuels techno-economic assessments. The experimental solar PV power production data have been obtained at the site of Forlì and Turin in Italy, Utrecht in Netherlands and in Almería in Spain. All the sites had a high temporal resolution leaving the possibility to analyze the influence of sub-hourly variation of PV power production. The e-fuel plant techno-economic assessment is done with a state-of-art investment and operation cost optimization model and simulated or experimental are used as input. By comparing the results, this study evaluates the influence of the time series simulation error bias on the e-fuel system design and fuel production costs using as an example, ammonia as a final product. One general conclusion of the analysis is that e-fuel project developers and modellers designing islanded e-fuel production system relying on simulated solar PV power should expect lower performances in reality. The results show that some PV power time series simulation tools provide accurate estimations, particularly during clear-sky days and periods of high-capacity factors. Conversely, they tend to overestimate production during low-capacity factor periods on cloudy days. These errors in PV production estimation can lead to significant error amplification

when used in the techno-economic assessment of e-fuel plants. Typically, overestimating solar resources results in an undersized hydrogen storage, electrolyser and power supply systems, and this effect is significantly amplified when the intermediate hydrogen storage is used seasonally. The tools and dataset tested leads to LCOF underestimation between 7 and 36.2 % with an average of 19.8 % across all sites (except Almería) and years, when the hydrogen end-user is constrained to run at full load all year. When the hydrogen end-user can operate only within a 40–100 % load range, the LCOF underestimation is between 6.3 and 25.3 % with an average of 14.5 %. For a completely flexible hydrogen end-user, the LCOF underestimation is between 0.8 and 17.4 % with an average of 8.5 %. None of the datasets or tools tested consistently outperform the others across different sites and years. In the specific case of Forlì with a flexible hydrogen end-user, it was found that using measured PV power time series instead of simulated ones is equivalent to overestimating the capital expenditure (CAPEX) of the PV plant or the electrolyzer by 56 %, the electrolyzer's electrical consumption by 58.5 %, or applying a discount rate (WACC) of 10.6 % instead of 8 %. This shows that the error inherent to using simulated PV power profiles instead of measured ones is likely to be higher than the one caused by other uncertainties for other parameters. The choice of the WACC is likely to give the same or higher order of error magnitude, as literature values usually vary between 4 and 10 %.

Further work should assess the impact of solar uncertainties across a wider range of locations and climates where high-quality measured power data is available. The newer and improved versions of the open-source PV power simulation tools should also be continuously tested in the future. To support this effort, an open-source collaborative repository was developed based on the work presented in this analysis. The repository provides open-source scripts for extracting simulated PV power profiles, conducting solar PV time series analysis, and performing green hydrogen techno-economic assessments using either simulated or measured solar PV power profiles [46,47]. Finally, follow-up research could focus on examining the impact of wind power generation uncertainties and analysing systems that combine both wind and solar power. Additionally, it could explore non-islanded systems that also include a grid connection.

Declaration of generative AI and AI-assisted technologies in the writing process

During the preparation of this work the authors used Chat GPT in order to correct grammar and syntax errors. After using this tool/service, the authors reviewed and edited the content as needed and take full responsibility for the content of the publication.

CRediT authorship contribution statement

Nicolas Campion: Conceptualization, Data curation, Formal analysis, Investigation, Methodology, Software, Validation, Visualization, Writing – original draft, Writing – review & editing. **Giulia Montanari:** Data curation, Formal analysis, Investigation, Methodology, Software, Validation, Visualization, Writing – original draft, Writing – review & editing. **Alessandro Guzzini:** Formal analysis, Resources, Validation, Writing – original draft, Writing – review & editing. **Lennard Visser:** Data curation, Resources, Writing – original draft, Writing – review & editing. **Alfredo Alcayde:** Data curation, Resources, Writing – original draft, Writing – review & editing.

Declaration of competing interest

The authors declare that they have no known competing financial interests or personal relationships that could have appeared to influence the work reported in this paper.

Acknowledgements

We thank our colleague Matti Koivisto and Juan Pablo Murcia Leon from DTU Wind and Energy system for their advices about the paper content and the use of the CorRES tool. Regarding the Italian case in Forlì, this study was also done in the framework of the research activities carried out within the Project “Network 4 Energy Sustainable Transition - NEST”, Spoke 7: Smart Sector Integration, Project code PE0000021, funded under the National Recovery and Resilience Plan (NRRP), Mission 4, Component 2, Investment 1.3 - Call for tender No. 1561 of October 11, 2022 of Ministero dell’Università e della Ricerca (MUR); funded by the European Union - NextGenerationEU. We also thank Marco Pellegrini and Cesare Saccani from the University of Bologna to give us access to the PV power solar production data in the site of Forlì in Italy and for their advices but also the Innovation and Development Department of HERA S.p.A that financed the design of the experimental plant and the acquisition of the real data. We thank Giovanni Carioni for his help for the extraction and the processing of the PV power production data in the site of Politecnico di Torino. This paper and related research have been conducted during and with the support of the Italian inter-university PhD course in sustainable development and climate change (link: www.phd-sdc.it).

Data availability

The original data and tools used for this study can be found at:
[OptiPlant \(Original data\)](#) (GitHub)
[Measured-vs-simulated-PV \(Original data\)](#) (GitHub)

References

- [1] Ueckerdt F, Bauer C, Dirnachner A, Everall J, Sacchi R, Luderer G. Potential and risks of hydrogen-based e-fuels in climate change mitigation. *Nat Clim Change* 2021;11:384–93. <https://doi.org/10.1038/s41558-021-01032-7>.
- [2] Svitnič T, Sundmacher K. Renewable methanol production: optimization-based design, scheduling and waste-heat utilization with the FluxMax approach. *Appl Energy* 2022;326:120017. <https://doi.org/10.1016/J.APENERGY.2022.120017>.
- [3] Kofler R, Clausen LR. Increasing carbon efficiency for DME production from wheat straw and renewable electricity – analysis of 14 system layouts. *Energy Convers Manag* 2023;281:116815. <https://doi.org/10.1016/J.ENCONMAN.2023.116815>.
- [4] Zhang H, Wang L, Van herle J, Maréchal F, Desideri U. Techno-economic comparison of green ammonia production processes. *Appl Energy* 2020;259:114135. <https://doi.org/10.1016/j.apenergy.2019.114135>.
- [5] Qi M, Kim M, Dat Vo N, Yin L, Liu Y, Park J, et al. Proposal and surrogate-based cost-optimal design of an innovative green ammonia and electricity co-production system via liquid air energy storage. *Appl Energy* 2022;314:118965. <https://doi.org/10.1016/j.apenergy.2022.118965>.
- [6] Campion N, Nami H, Swisher PR, Vang Hendriksen P, Münster M. Techno-economic assessment of green ammonia production with different wind and solar potentials. *Renew Sustain Energy Rev* 2023;173. <https://doi.org/10.1016/j.rser.2022.113057>.
- [7] Ikäheimo J, Kiviluoma J, Weiss R, Holttinen H. Power-to-ammonia in future North European 100 % renewable power and heat system. *Int J Hydrogen Energy* 2018;43:17295–308. <https://doi.org/10.1016/j.ijhydene.2018.06.121>.
- [8] Lester MS, Bramstoft R, Münster M. Analysis on electrofuels in future energy systems: a 2050 case study. *Energy* 2020;199:117408. <https://doi.org/10.1016/j.energy.2020.117408>.
- [9] Bramstoft R, Pizarro-Alonso A, Jensen IG, Ravn H, Münster M. Modelling of renewable gas and renewable liquid fuels in future integrated energy systems. *Appl Energy* 2020;268:114869. <https://doi.org/10.1016/j.apenergy.2020.114869>.
- [10] Welder L, Ryberg DS, Kotzur L, Grube T, Robinius M, Stolten D. Spatio-temporal optimization of a future energy system for power-to-hydrogen applications in Germany. *Energy* 2018;158:1130–49. <https://doi.org/10.1016/J.ENERGY.2018.05.059>.
- [11] Colbertaldo P, Guandalini G, Campanari S. Modelling the integrated power and transport energy system: the role of power-to-gas and hydrogen in long-term scenarios for Italy. *Energy* 2018;154:592–601. <https://doi.org/10.1016/J.ENERGY.2018.04.089>.
- [12] Kountouris I, Bramstoft R, Madsen T, et al. A unified European hydrogen infrastructure planning to support the rapid scale-up of hydrogen production. *Nat Commun* 2024;15:5517. <https://doi.org/10.1038/s41467-024-49867-w>.
- [13] Bhandari R, Shah RR. Hydrogen as energy carrier: techno-economic assessment of decentralized hydrogen production in Germany. *Renew Energy* 2021;177:915–31. <https://doi.org/10.1016/J.RENENE.2021.05.149>.
- [14] Mazzeo D, Herdem MS, Matera N, Wen JZ. Green hydrogen production: analysis for different single or combined large-scale photovoltaic and wind renewable systems. *Renew Energy* 2022;200:360–78. <https://doi.org/10.1016/J.RENENE.2022.09.057>.
- [15] Fasihi M, Weiss R, Savolainen J, Breyer C. Global potential of green ammonia based on hybrid PV-wind power plants. *Appl Energy* 2021;294:116170. <https://doi.org/10.1016/J.APENERGY.2020.116170>.
- [16] Osmar O, Sgouridis S, Sleptchenko A. Scaling the production of renewable ammonia: a techno-economic optimization applied in regions with high insolation. *J Clean Prod* 2020;271. <https://doi.org/10.1016/j.jclepro.2020.121627>.
- [17] Armijo J, Philibert C. Flexible production of green hydrogen and ammonia from variable solar and wind energy: case study of Chile and Argentina. *Int J Hydrogen Energy* 2020;45:1541–58. <https://doi.org/10.1016/j.ijhydene.2019.11.028>.
- [18] Salmon N, Bañares-Alcántara R. Green ammonia as a spatial energy vector: a review. <https://doi.org/10.1039/dlse00345c>; 2021.
- [19] Staffell I, Pfenniger S. Renewables ninja. <https://www.renewables.ninja/>; 2019.
- [20] Arnaiz del Pozo C, Cloete S. Techno-economic assessment of blue and green ammonia as energy carriers in a low-carbon future. *Energy Convers Manag* 2022;255:115312. <https://doi.org/10.1016/j.enconman.2022.115312>.
- [21] NASA. Surface meteorology and solar energy (SSE). https://ntrs.nasa.gov/citation_s/20080012200. [Accessed 29 March 2023].
- [22] Salmon N, Bañares-Alcántara R. Impact of grid connectivity on cost and location of green ammonia production: Australia as a case study. *Energy Environ Sci* 2021;14:6655–71. <https://doi.org/10.1039/d1ee02582a>.
- [23] Nayak-Luke RM, Bañares-Alcántara R. Techno-economic viability of islanded green ammonia as a carbon-free energy vector and as a substitute for conventional production. *Energy Environ Sci* 2020;13:2957–66. <https://doi.org/10.1039/d0ee01707h>.
- [24] Meteonorm. *Meteonorm software* 2023.
- [25] Sánchez A, Martín M. Optimal renewable production of ammonia from water and air. *J Clean Prod* 2018;178:325–42. <https://doi.org/10.1016/J.JCLEPRO.2017.12.279>.
- [26] Junta de Andalucía. Solar Radiation n.d <https://www.agenciaandaluzadelaenergia.es/Radiacion/radiacion2.php>.
- [27] Qi M, Vo DN, Yu H, Shu CM, Cui C, Liu Y, et al. Strategies for flexible operation of power-to-X processes coupled with renewables. *Renew Sustain Energy Rev* 2023;179:113282. <https://doi.org/10.1016/J.RSER.2023.113282>.
- [28] Arnaiz del Pozo C, Cloete S, Jiménez Álvaro Á. Techno-economic assessment of long-term methanol production from natural gas and renewables. *Energy Convers Manag* 2022;266:115785. <https://doi.org/10.1016/J.ENCONMAN.2022.115785>.
- [29] Sengupta M, Xie Y, Lopez A, Habte A, Maclaurin G, Shelby J. The national solar radiation data base (NSRDB). *Renew Sustain Energy Rev* 2018;89:51–60. <https://doi.org/10.1016/J.RSER.2018.03.003>.
- [30] Terlouw T, Bauer C, McKenna R, Mazzotti M. Large-scale hydrogen production via water electrolysis: a techno-economic and environmental assessment. *Energy Environ Sci* 2022;15:3583–602. <https://doi.org/10.1039/d2ee01023b>.
- [31] Huld T, Müller R, Gambardella A. A new solar radiation database for estimating PV performance in Europe and Africa. *Sol Energy* 2012;86:1803–15. <https://doi.org/10.1016/J.SOLENER.2012.03.006>.
- [32] Al-Ghassian L, Ahmad AD, Abubaker AM, Hovi K, Hassan MA, Annuk A. Techno-economic feasibility of hybrid PV/wind/battery/thermal storage trigeneration system: toward 100% energy independency and green hydrogen production. *Energy Rep* 2023;9:752–72. <https://doi.org/10.1016/j.egyr.2022.12.034>.
- [33] Khan MHA, Heywood P, Kuswara A, Daiyan R, MacGill I, Amal R. An integrated framework of open-source tools for designing and evaluating green hydrogen production opportunities. *Commun Earth Environ* 2022;3:1–18. <https://doi.org/10.1038/s43247-022-00640-1>.
- [34] Hofrichter A, Rank D, Heberl M, Sternier M. Determination of the optimal power ratio between electrolysis and renewable energy to investigate the effects on the hydrogen production costs. *Int J Hydrogen Energy* 2023;48:1651–63. <https://doi.org/10.1016/J.IJHYDENE.2022.09.263>.
- [35] Raab M, Körner R, Dietrich RU. Techno-economic assessment of renewable hydrogen production and the influence of grid participation. *Int J Hydrogen Energy* 2022;47:26798–811. <https://doi.org/10.1016/J.IJHYDENE.2022.06.038>.
- [36] Marocco P, Gandiglio M, Santarelli M. Optimal design of PV-based grid-connected hydrogen production systems. *J Clean Prod* 2023;140007. <https://doi.org/10.1016/J.JCLEPRO.2023.140007>.
- [37] Dufo-López R, Lujano-Rojas JM, Bernal-Agustín JL. Optimisation of size and control strategy in utility-scale green hydrogen production systems. *Int J Hydrogen Energy* 2024;50:292–309. <https://doi.org/10.1016/J.IJHYDENE.2023.08.273>.
- [38] NASA. NASA POWER | prediction of worldwide energy resources. <https://power.larc.nasa.gov/>. [Accessed 27 August 2024].
- [39] Staffell I, Pfenniger S. Using bias-corrected reanalysis to simulate current and future wind power output. *Energy* 2016;114:1224–39. <https://doi.org/10.1016/j.energy.2016.08.068>.
- [40] Pfenniger S, Staffell I. Long-term patterns of European PV output using 30 years of validated hourly reanalysis and satellite data. *Energy* 2016;114:1251–65. <https://doi.org/10.1016/j.energy.2016.08.060>.
- [41] Muñoz Ortiz M, Kvalbein L, Hellemo L. Evaluation of open photovoltaic and wind production time series for Norwegian locations. *Energy* 2021;236:121409. <https://doi.org/10.1016/J.ENERGY.2021.121409>.
- [42] Tahir Z ul R, Amjad M, Asim M, Azhar M, Farooq M, Ali MJ, et al. Improving the accuracy of solar radiation estimation from reanalysis datasets using surface measurements. *Sustain Energy Technol Assessments* 2021;47:101485. <https://doi.org/10.1016/J.SETA.2021.101485>.

- [43] Gualtieri G. Analysing the uncertainties of reanalysis data used for wind resource assessment: a critical review. *Renew Sustain Energy Rev* 2022;167:112741. <https://doi.org/10.1016/J.RSER.2022.112741>.
- [44] Kies A, Schyska BU, Bilousova M, El Sayed O, Jurasz J, Stoecker H. Critical review of renewable generation datasets and their implications for European power system models. *Renew Sustain Energy Rev* 2021;152:111614. <https://doi.org/10.1016/J.RSER.2021.111614>.
- [45] Mathews D, Ó Gallachóir B, Deane P. Systematic bias in reanalysis-derived solar power profiles & the potential for error propagation in long duration energy storage studies. *Appl Energy* 2023;336:120819. <https://doi.org/10.1016/J.APENERGY.2023.120819>.
- [46] Montanari G. giumonros/Measured-vs-simulated-PV. <https://github.com/giumonros/Measured-vs-simulated-PV>. [Accessed 18 October 2024].
- [47] Campion N GitHub - njbca/OptiPlant: Optiplant is a linear optimization model that minimize the investment and operation costs of a power-to-X system that can be powered with wind, solar and the grid 2023. <https://github.com/njbca/OptiPlant/> (accessed June 3, 2024).
- [48] World Bank. Global Solar Atlas n.d <https://globalsolaratlas.info/map>.
- [49] Beck HE, McVicar TR, Vergopolan N, Berg A, Lutsko NJ, Dufour A, et al. High-resolution (1 km) Köppen-Geiger maps for 1901–2099 based on constrained CMIP6 projections. *Sci Data* 2023 101 2023;10:1–16. <https://doi.org/10.1038/s41597-023-02549-6>.
- [50] Köppen-Geiger Explorer n.d <https://koppene.earth> (accessed July 16, 2024).
- [51] Visser LR, Elsinga B, Alskiaf TA, Van Sark WGJHM. Open-source quality control routine and multi-year power generation data of 175 PV systems. *J Renew Sustain Energy* 2022;14:43501. <https://doi.org/10.1063/5.0100939/2848635>.
- [52] Bianchini A, Gambuti M, Pellegrini M, Saccani C. Performance analysis and economic assessment of different photovoltaic technologies based on experimental measurements. *Renew Energy* 2016;85:1–11. <https://doi.org/10.1016/j.renene.2015.06.017>.
- [53] Viciana E, Arrabal-Campos FM, Alcayde A, Baños R, Montoya FG. All-in-one three-phase smart meter and power quality analyzer with extended IoT capabilities. *Measurement* 2023;206:112309. <https://doi.org/10.1016/J.MEASUREMENT.2022.112309>.
- [54] Koivisto M, Das K, Guo F, Sørensen P, Nuño E, Cutululis N, et al. Using time series simulation tools for assessing the effects of variable renewable energy generation on power and energy systems. *Wiley Interdiscip Rev Energy Environ* 2019;8:1–15. <https://doi.org/10.1002/wene.329>.
- [55] Rienecker MM, Suarez MJ, Gelaro R, Todling R, Bacmeister J, Liu E, et al. MERRA: NASA's Modern-Era Retrospective analysis for research and applications. *J Clim* 2011;24:3624–48. <https://doi.org/10.1175/JCLI-D-11-00015.1>.
- [56] Müller R, Pfeifroth U, Träger-Chatterjee C, Trentmann J, Cremer R. Digging the METEOSAT treasure—3 decades of solar surface radiation. *Rem Sens* 2015;7:8067–101. <https://doi.org/10.3390/RS70608067>. 2015;7:8067–101.
- [57] Hersbach H, Bell B, Berrisford P, Hirahara S, Horányi A, Muñoz-Sabater J, et al. The ERA5 global reanalysis. *Q J R Meteorol Soc* 2020;146:1999–2049. <https://doi.org/10.1002/QJ.3803>.
- [58] Huld T, Gottschalg R, Beyer HG, Topic M. Mapping the performance of PV modules, effects of module type and data averaging. *Sol Energy* 2010;84:324–38. <https://doi.org/10.1016/J.SOLENER.2009.12.002>.
- [59] Dobos A. PVWatts version 5 manual - technical report NREL/TP-6A20-62641, vol. 20. Natl Renew Energy Lab; 2014.
- [60] Lettoff A, Campion N, Böhme M, Jensen CD, Ahrenfeldt J, Clausen LR. Techno-economic assessment of upgraded pyrolysis bio-oils for future marine fuels. *Energy Convers Manag* 2024;306:118225. <https://doi.org/10.1016/J.ENCONMAN.2024.118225>.
- [61] Kofler R, Campion N, Hillestad M, Meesenburg W, Clausen LR. Techno-economic analysis of dimethyl ether production from different biomass resources and off-grid renewable electricity. *Energy Fuel* 2024;38:8777–803. https://doi.org/10.1021/ACS.ENERGYFUELS.4C00311/SUPPL_FILE/EF4C00311_SI_001.PDF.
- [62] Osman O, Sgouridis S, Sleptchenko A. Scaling the production of renewable ammonia: a techno-economic optimization applied in regions with high insolation. *J Clean Prod* 2020;271:121627. <https://doi.org/10.1016/j.jclepro.2020.121627>.
- [63] Papadias DD, Ahalwalia RK. Bulk storage of hydrogen. *Int J Hydrogen Energy* 2021;46:34527–41. <https://doi.org/10.1016/J.IJHYDENE.2021.08.028>.
- [64] IRENA. Electricity storage and renewables: costs and markets to 2030. 2017.
- [65] DEA. Technology data energy storage. 2020.
- [66] Yi Y, Kimball JS, Jones LA, Reichle RH, McDonald KC. Evaluation of MERRA land surface estimates in preparation for the soil moisture active passive mission. *J Clim* 2011;24:3797–816. <https://doi.org/10.1175/2011JCLI4034.1>.
- [67] Boilley A, Wald L. Comparison between meteorological re-analyses from ERA-Interim and MERRA and measurements of daily solar irradiation at surface. *Renew Energy* 2015;75:135–43. <https://doi.org/10.1016/J.RENENE.2014.09.042>.
- [68] Mukherjee A, Bruijninx P, Junginger M. Techno-economic competitiveness of renewable fuel alternatives in the marine sector. *Renew Sustain Energy Rev* 2023;174:113127. <https://doi.org/10.1016/J.RSER.2022.113127>.
- [69] Bellotti D, Rivarolo M, Magistri L. A comparative techno-economic and sensitivity analysis of Power-to-X processes from different energy sources. *Energy Convers Manag* 2022;260:115565. <https://doi.org/10.1016/j.enconman.2022.115565>.
- [70] Wang C, Walsh SDC, Longden T, Palmer G, Lutalo I, Dargaville R. Optimising renewable generation configurations of off-grid green ammonia production systems considering Haber-Bosch flexibility. *Energy Convers Manag* 2023;280:116790. <https://doi.org/10.1016/J.ENCONMAN.2023.116790>.
- [71] Technology Data | Energystyrelsen n.d <https://ens.dk/en/our-services/projections-and-models/technology-data> (accessed September 11, 2023).
- [72] Irena. Renewable generation costs in 2022. 2022.
- [73] International Renewable Energy Agency. Green hydrogen cost reduction: scaling up electrolyzers to meet the 1.5C climate goal. 2020. Abu Dhabi.